Study of Integrin CD11b's Regulation on Mincle signaling

Quanri Zhang

The Graduate School

Yonsei University

Department of Integrated Omics

for Biomedical Science

Study of Integrin CD11b's Regulation on Mincle signaling

A Dissertation

Submitted to the Department of Integrated Omics for

Biomedical Science

And the Graduate School of Yonsei University

In partial fulfillment of the

Requirements for the degree of

Doctor of Philosophy

Quanri Zhang

December 2016

This certifies that the dissertation of Quanri Zhang
is approved.

Thesis Supervisor: Young-Joon Kim

Thesis Committee Member : Bo-Youn Park

Thesis Committee Member : Han-Woong Lee

Thesis Committee Member : Sang-Jun Ha

Thesis Committee Member : Nam-On Ku

The Graduate School
Yonsei University
December 2016

Table of contents

Page

List of Figures

List of Tables

Abbreviation

TDM : trehalose-6,6-dimycolate

Mincle : macrophage inducible Ca^{2+}-dependent lectin

BCG : Bacillus Calmette–Guérin

NO : nitric oxide

LPS : lipopolysaccharide

BMDM : bone-marrow-derived macrophage

DC : dendritic cell

iBMM : immortalized BMM

PLA : Proximity ligation assay

Abstract

Study of Integrin CD11b's Regulation on Mincle signaling

Quanri Zhang

Department of Integrated Omics

for Biomedical Science

The Graduate School

Yonsei University

During mycobacteria infection, anti-inflammatory responses allow the host to avoid tissue damage caused by overactivation of the immune system; however, little is known about the negative modulators that specifically control mycobacteria-induced immune responses. Here, we demonstrate that integrin CD11b is a critical negative regulator of mycobacteria cord factor-induced macrophage-inducible C-type lectin (Mincle) signaling. CD11b deficiency resulted in hyperinflammation following mycobacterial infection. Activation of Mincle by mycobacterial components turns on not only the Syk signaling pathway but also CD11b signaling, and induces formation of a Mincle-CD11b signaling complex. The activated CD11b recruits Lyn, SIRPα, and SHP1, which dephosphorylate Syk to inhibit Mincle-mediated inflammation. Furthermore, the Lyn activator MLR1023 effectively suppressed Mincle signaling, indicating the possibility of Lyn-mediated control of

inflammatory responses. These results describe a new role for CD11b in fine-tuning the immune response against mycobacterium infection.

Key words: Mycobacteria, CD11b, Mincle, Lyn-Sirpα-Shp1 complex

1. Introduction

The hallmark of *Mycobacterium tuberculosis* (Mtb) infection is the formation of a granuloma, a compact aggregate of immune cells[1]. The granuloma has been thought to function as a host defense mechanism to prevent further spread of Mtb; however, recent studies suggest that the granuloma can also shelter the bacteria and ensure persistence of these organisms in a latent form[2, 3]. Therefore, clearance of the mycobacteria that persist in the granuloma is required for efficient clearance of the infection.

Granuloma formation is initiated by an orchestrated production of cytokines and chemokines coupled with the upregulation of selectins and integrins on immune cells to recruit and activate different populations of leukocytes[4]. As granuloma formation progresses, the intense proinflammatory responses are suppressed by negative modulators, to prevent excessive granuloma formation[5]. The most prominent anti-inflammatory cytokine involved in the downregulation of granuloma formation is interleukin (IL)-10, which antagonizes the activity of IL-17 and interferon (IFN)-γ, thereby lessening the protective immune responses of macrophages[6, 7] . Additionally, IL-10 may inhibit antigen presentation by dendritic cells (DCs) via blockade of major histocompatibility complex molecules[8]. This compromised immune environment may, therefore, enable the bacteria to evade host immune surveillance and survive for a long time in the lungs, ultimately leading to a chronic infection. Hence, understanding the protective mechanism of negative regulators of granuloma formation will elucidate key targets for the development of immune therapies to fight Mtb infection.

Mtb carries diverse pathogen-associated molecular patterns (PAMPs) that can initiate an inflammatory response in the host. Among these PAMPs, the virulent cord factor trehalose-6,6-dimycolate (TDM) is specifically recognized by macrophage-inducible C-type lectin (Mincle), and this cord factor alone leads to a granulomatous response through the robust production of nitric oxide (NO) and various proinflammatory cytokines and chemokines, including IL-6, tumor necrosis factor (TNF)-α, and monocyte chemoattractant protein (MCP)-1[9, 10, 11]. Additionally, TDM stimulation critically enhances the cellular adhesion of neutrophils by increasing their surface expression of integrin CD11b/CD18[12]. Amplified integrin surface expression allows neutrophils to infiltrate into and accumulate around infected sites, enabling recruitment of additional neutrophils to kill the bacteria. Thus, Mincle appears to play a key role in the fight of leukocytes against mycobacteria infection. While the activation of the proinflammatory response by Mincle has been studied extensively, the negative mediators that specifically restrain Mincle signaling during granuloma formation remain to be elucidated.

The integrin heterodimer CD11b/CD18 mainly functions in cell adhesion and migration during inflammation[13]. Intriguingly, recent studies in CD11b-deficient mice suggest a broad crosstalk between CD11b and various pattern recognition receptor (PRR)-mediated pathways. Specifically, CD11b activated by Toll-like receptor 4 (TLR4) signaling targets Myd88 and TIR domain-containing adapter-inducing interferon-β (TRIF) for proteasome degradation, thereby negatively regulating the TLR4 signal in peripheral macrophages[14]. Moreover, CD11b can interfere with the function of T and B cells by suppressing the differentiation of T_H17 cells and inhibiting B cell receptor (BCR) signaling[15, 16]. Considering that CD11b is

upregulated in TDM-activated neutrophils and plays a role in the negative regulation of TLR signaling, the relatively static function of macrophages in the granuloma may result from the negative regulation of Mincle by CD11b during granuloma formation.

In the present study, we demonstrate that TDM-challenged CD11b-deficient mice developed more severe granulomas with increased recruitment of leukocytes and increased production of proinflammatory cytokines. In macrophages, the absence of CD11b led to increased cytokine production and release of NO and reactive oxygen species (ROS) upon TDM stimulation, as well as to enhanced cytokine production against *Mycobacterium bovis* Bacillus Calmette-Guérin (BCG) infection. With respect to neutrophils, CD11b was indispensable for adhesion, and CD11b deficiency resulted in increased cytokine levels. We found that activated CD11b formed a signaling complex with activated Mincle that recruited Lyn kinase, SIRPα, and SHP1; this complex regulated the phosphorylation of the Mincle downstream target Syk, thereby suppressing Mincle-dependent inflammatory responses. Therefore, CD11b functions as a negative modulator of TDM-Mincle signaling by dephosphorylating Syk kinase via the Lyn-SIRPα-SHP1 complex.

2. Materials and methods

2.1. Animals

C57BL/6 mice, aged 6–7 weeks, were purchased from Orient Bio. $CD11^{-/-}$ mice were obtained from Jackson Laboratory, and $Mincle^{-/-}$ mice (Clec4eMNA) were obtained from the Consortium for Functional Glycomics. The animals were backcrossed for nine generations onto the C57BL/6 background. All mice were maintained in a specific pathogen-free facility at the Laboratory Animal Research Center at Yonsei University. Protocols were approved by the Institutional Animal Care and Use Committees of the Laboratory Animal Research Center at Yonsei University (permit number: IACUC-A-201410-317-01).

2.2. Cell culture

BMMs were prepared by culturing BM cells with 20% (v/v) L929 culture supernatant in basic Dulbecco's modified Eagle medium (DMEM; ThermoFisher Scientific) supplemented with 20% fetal bovine serum (FBS; Gibco/ThermoFisher Scientific), 50 U/ml penicillin, and 50 mg/ml streptomycin for 7 days. BMDCs were differentiated by culturing BM cells with 15 ng/ml recombinant granulocyte-macrophage colony-stimulating factor (rGM-CSF) in DMEM for 10 days. BM neutrophils were purified directly from BM cells by 53/63/76% three-layer Percoll gradient centrifugation as described[12] and cultured in RPMI basic medium supplemented with 10% FBS and penicillin/streptomycin. The iBMM cell line was obtained from BEI Resources (no. NR-9456).

For TDM stimulation, 50 μg/ml TDM (Sigma) was added to culture plates before cell plating. Cells were primed with 10 ng/ml IFN-γ (Pierce), 100 ng/ml Pam3CSK4 (InvivoGen), and 10 ng/ml ultrapure LPS (InvivoGen) for the indicated times. For the inhibitor assay, the indicated inhibitors were added 30 min before stimulation. PP1 (Src family kinase inhibitor, 529579, 5 μM), PP2 (Src family kinase inhibitor, 529573, 100 nM), Syk Inhibitor (574711, 10 μM), and SB203580 (559389, 10 μM) were purchased from CalBiochem. AG490 (T3434, 25 μM) and SP600125 (S5567, 10 μM) were obtained from Sigma. Parthenolide (0610, 5 μM), U0126 (1144, 10 μM) and wortmannin (1232, 10 μM) were purchased from Tocris. The Lyn activator MLR1023 (4582, 1 ng/ml) was also purchased from Tocris. Fibrinogen from Sigma (F3879, 15 μg/ml) was diluted in PBS and coated on plates at 4°C overnight. Then, the fibrinogen was aspirated and the plate was washed three times with PBS before cell plating.

2.3. ELISA, immunoblot analysis, and immunoprecipitation

IL-6 and TNF-α secretion in culture supernatants was measured using an enzyme-linked immunosorbent assay (ELISA) kit (Biolegend). For immunoblot analysis, cells were lysed for 15 min at 4°C in RIPA lysis buffer (100 mM Tris-HCl, pH 8.0, 50 mM NaCl, 5 mM EDTA, 0.5% NP-40, 1% Triton X-100, 50 mM β-glycerophosphate, 50 mM NaF, 0.1 mM Na_3VO_4, and 0.5% sodium deoxycholate) with protease inhibitor cocktail (Roche). Following lysis, suspensions were centrifuged at 1,300 × *g* for 15 min at 4°C to remove nuclei. Then, proteins were separated by SDS-PAGE and transferred to nitrocellulose membranes. The membranes were developed with Amersham enhanced chemiluminescence (ECL) reagents, followed by detection of the signal using the ImageQuant LAS 4000 system (GE Healthcare). For

immunoprecipitation assays, cells were stimulated with TDM for the indicated times. Then, cells were washed and resuspended in NP-40 lysis buffer [50 mM Tris-HCl, pH 7.5, 1 mM EGTA, 1 mM EDTA, pH 8.0, 50 mM NaF, 1 mM sodium glycerophosphate, 5 mM pyrophosphate, 0.27 M sucrose, 0.5% NP-40, 0.1 mM phenylmethylsulfonyl fluoride (PMSF), 0.1% 2-mercaptoethanol, 1 mM Na_3VO_4, and protease inhibitor cocktail (Roche)]. After removing nuclei by centrifugation at 1,300 × *g* for 15 min at 4°C, the cell extracts were incubated with V5 agarose or agarose-A beads with Lyn or SHP1 antibodies overnight at 4°C. After pull-down, the agarose was washed three times in ice-cold lysis buffer and proteins were eluted by boiling in SDS sample buffer. The precipitated proteins were subjected to immunoblot analysis as described above. The antibodies used in this study are listed in Supplementary Table 1.

2.4. Adhesion assay

Neutrophils (3×10^5 cells/well) were labeled by incubation with 5 μg/ml calcein-acetoxymethyl ester at 37°C for 30 min, washed with PBS, and resuspended in RPMI medium containing 10% FBS. Cells were then plated in 48-well tissue culture plates for TDM stimulation. After 6 h of adhesion, non-adherent cells were washed away with PBS aspiration, and adherent cells were imaged under a fluorescent microscope. The percentage of adherent cells was determined by comparison of fluorescence measured by a microplate reader (Tecan Infinite Pro 200) at 492 nm before and after washing.

2.5. ROS assay

ROS production was measured with carboxy-H_2DCFDA dye (Molecular Probes). Macrophages (3×10^5 cells/well) and neutrophils (1×10^5 cells/well) were seeded in 96-well plates and pre-incubated with 10 μM H_2DCFDA in PBS for 30 min. After washing in PBS, cells were stimulated with TDM. After 6 and 18 h of treatment, oxidized DCFDA was analyzed at 495 nm/520 nm using a Multilabel Plate Reader (Victor5, Perkin Elmer). The data were normalized to the negative control, which consisted of unchallenged cells.

2.6. NO measurement

NO concentration was measured by classic colorimetric Griess reaction[17]. Culture supernatants were incubated with an equal volume of Griess reagent (Sigma-Aldrich, G4410) for 5 min at RT. The absorbance was determined at 570 nm with a Perkin Elmer 550 S spectrophotometer. Prepared sodium nitric oxide (1–100 μM) was used to generate a standard curve for calculating sample NO concentrations.

2.7. Site-directed mutagenesis

The SHP1 D419A and C453S dominant-negative mutants were constructed using a site-directed mutagenesis kit (Stratagene) according to the manufacturer's instructions. Primers used are listed in Supplementary Table 2.

2.8. TDM-induced pulmonary granulomas

To elicit pulmonary granuloma formation, 9–11-week-old mice were injected intravenously through the tail vein with 100 μl of a water-in-oil emulsion containing 100 μg of TDM (Sigma). On day 7 post-challenge, mice were sacrificed, lungs were weighed, and the LWI was calculated as described previously[18, 19]. A portion of the fresh lung was subjected to flow cytometry to assess the leukocyte infiltration just after sacrifice. The large lobe of the right lung was fixed in 10% formaldehyde for hematoxylin and eosin staining. Other lung sections were homogenized and frozen for future analysis by ELISA or qRT-PCR.

2.9. Air pouch model

Briefly, air pouches were established on the dorsal sides of 9–10-week-old WT and $CD11b^{-/-}$ mice by subcutaneous injection of 3 ml of sterile air on day 0. A second injection of 1.5 ml of sterile air into the pouch was performed on day 3. On day 7, 200 μl of a water-in-oil emulsion containing 50 μg of TDM was injected into the pouch cavity, while an emulsion without TDM was injected into the control animals. Approximately 24 h after the final injection, mice were sacrificed, and the pouch cavities were washed with PBS. The wash fluid was harvested for leukocyte population analysis by flow cytometry and cytokine measurement by ELISA.

2.10. Flow cytometric analysis

A portion of the lungs was weighed, incubated in 2 mg/ml collagenase D (Roche) and 40 U/ml DNase I (Roche), and dispersed by passage through 70 mm mesh. After red blood cell lysis, viable cells were counted and incubated with fluorescence-conjugated antibodies for

labeling. The following specific FACS antibodies (BD Pharmingen) were used: Gr-1 (RB6-8C5), CD11b (M1/70), Ly6G (1A8), CD3e (145-2C11), and CD19 (1D3). To determine CD11b and CD18 expression on neutrophils, purified neutrophils were incubated with anti-mouse CD11b (M1/70) and CD18 (C71/16) (BD Pharmingen). After incubation, cells were analyzed on a FACS Calibur instrument (BD Biosciences). The isotype control antibodies used in this experiment were obtained from BD Pharmingen.

2.11. In situ PLA

Protein-protein interactions were investigated using the Duolink *In Situ* Red Starter Kit (Sigma, DUO92105) according to the manufacturer's instructions. Immortalized BMMs were transfected using Lipofectamine for 24 h, and 1×10^3 cells in 200 μl of medium were seeded onto 8-well chamber slides coated with TDM. After 24 h, cells were fixed in 4% paraformaldehyde for 15 min. Fluorescence was detected with a LSM 700 (Zeiss) confocal microscope, and signal intensities were quantified with Photoshop CS. Antibodies used in the PLA assay are listed in Supplementary Table 1.

2.12. CRISPR-Cas9-dependent gene knockout in iBMM cells

For knockout in iBMM cells, single-strand guide RNAs were annealed to form gRNA oligo duplexes and then ligated into digested lentiCRISPR v2 vectors (Addgene plasmid #52961; a gift from Feng Zhang). Lentivirus was generated by co-transfecting HEK 293FT cells with lentiCRISPR v2, psPAX2 (packaging), and pMD2.G (envelope). After 48 h, virus-containing supernatants were collected and added onto the iBMM cells along with polybrene (8 μg/ml,

Sigma). Cells were selected with puromycin (2 μg/ml), and single-cell colonies were further selected by plating in 96-well plates. Gene knockout colonies were validated by immunoblot. Colonies that still expressed the target proteins were used as negative control lines.

2.13. BCG infection

Macrophages were seeded in 48-well plates (2.0×10^5 cells/well) and incubated overnight. Cells were then infected with BCG at a MOI of 10 for 4 h. Non-internalized bacteria were washed away with PBS, and cells were incubated with fresh DMEM. At 24, 48, and 72 h after infection, media was collected for the analysis of cytokine levels by ELISA.

2.14. qRT-PCR

Total RNA from cells and tissues was extracted with TRIzol reagent (ThermoFisher Scientific) according to the manufacturer's instructions. Then, cDNA was synthesized using SuperScript II reverse transcriptase (ThermoFisher Scientific) with oligo(dT) primers. Expression of individual genes was determined by real-time PCR using a Bio-Rad CFX and quantified by normalizing to the housekeeping gene *Gapdh* by the change-in-cycling-threshold ($\Delta\Delta C_T$) method. Primers used are listed in Supplementary Table 2.

2.15. Statistical analysis

Software Prism 6.0 (GraphPad) was used to run unpaired two-tailed *t*-tests with a 95% confidence interval for the calculation of *P*-values.

3. Results

3.1. Increased cytokine production against mycobacteria in CD11b-deficient mice

To examine the involvement of the integrin receptor in anti-mycobacterial infection, bone marrow-derived macrophages (BMMs) from wild-type (WT), CD11b-deficient ($CD11b^{-/-}$), and Mincle-deficient ($Mincle^{-/-}$) mice were challenged with BCG. BCG infection of WT BMMs induced the secretion of high levels of inflammatory cytokines such as IL-6 and TNF-α (**Fig. 1a**); however, $Mincle^{-/-}$ BMMs were defective in the secretion of these cytokines in response to BCG treatment, indicating that Mincle is the major PRR that mediates cytokine release during BCG infection. By contrast, CD11b deficiency caused hyperinduction of inflammatory cytokines in response to BCG treatment, indicating that CD11b exerts an inhibitory effect on anti-mycobacterial immune signaling. Because CD11b is known to mediate inflammation by regulating leukocyte adhesion[20], we asked whether the defective cellular adhesion in CD11b-deficient BMMs is responsible for the abnormal production of cytokines. To this end, we compared the phagocytosis efficiencies of WT and mutant BMMs using fluorescent beads. Interestingly, all BMMs tested exhibited comparable phagocytic ability, even in the presence of TDM-coated particles (**Fig. 2**). Together, these results indicate that CD11b deficiency may affect anti-mycobacterial cytokine production via effects on signaling rather than cell adhesion.

3.2. Enhanced TDM-Mincle signaling in CD11b-deficient macrophages

Because TLR signaling is independent of CD11b in BMMs[21], the hyperinduction of inflammatory cytokines in CD11b-deficient BMMs upon BCG infection appeared to mainly be dependent on Mincle, which recognizes the major cell wall component of BCG. Thus, we investigated the potential role of CD11b in the direct regulation of Mincle using a Mincle-specific ligand, TDM. TDM stimulation caused greater production of IL-6 and TNF-α in $CD11b^{-/-}$ BMMs than in WT BMMs (**Fig. 1b**). The disparity between the WT and the $CD11b^{-/-}$ phenotype was further increased when the macrophages were primed with IFN-γ. Therefore, the hyperinflammatory cytokine production in response to BCG in the CD11b-deficient BMMs appeared to have resulted from abnormal regulation of the Mincle signaling pathway.

To confirm the effect of CD11b deletion on Mincle signaling, we examined the expression of key molecules that are specifically regulated by Mincle, such as inducible nitric oxide synthase (iNOS) and Cox-2[22]. Indeed, iNOS and Cox-2 were highly expressed in the TDM-stimulated $CD11b^{-/-}$ macrophages, while expression of these factors was not detectable in the TDM-stimulated WT BMMs. These discrepancies were further increased under IFN-γ-primed conditions that induced high Mincle expression (**Fig. 1c**). Consistently, NO and NADPH oxidase-dependent ROS were produced at higher levels in $CD11b^{-/-}$ macrophages than in WT macrophages upon TDM stimulation (**Fig. 1d, e**). Measurement of mRNA by quantitative reverse transcription-coupled polymerase chain reaction (qRT-PCR) revealed that diverse inflammatory cytokines (*Il6*, *Tnf*, *Il1a*, and *Il1b*), chemokines (*Ccl2*, *Cxcl2*, and

Cxcl10), and signaling molecules (*Nos2* and *Mmp3*), as well as anti-inflammatory cytokines (*Il10* and *Ifnb*), were highly upregulated in the CD11b$^{-/-}$ macrophages (**Fig. 3**).

To further examine the involvement of CD11b in Mincle signaling, the activation of molecules downstream of Mincle was monitored. TDM stimulation induced extracellular signal-regulated kinase (Erk)1/2 and spleen tyrosine kinase (Syk) phosphorylation specifically, and the activation of these molecules was further enhanced in CD11b$^{-/-}$ BMMs compared with WT BMMs (**Fig. 1f**). To rule out the possibility of Mincle-dependent kinase activation via positive feedback due to higher Mincle expression in CD11b$^{-/-}$ macrophages, WT and CD11b$^{-/-}$ macrophages were primed with TLR agonists to induce similar levels of Mincle expression, as described previously[23]. Both lipopolysaccharide (LPS) and Pam3, a TLR2 agonist, induced a similar level of Mincle protein expression, and both stimuli failed to induce Syk or Erk1/2 phosphorylation in the absence of TDM treatment. TDM treatment of the primed BMMs, however, activated Syk and Erk1/2 phosphorylation robustly, with significantly stronger activation in the CD11b$^{-/-}$ BMMs than in the WT cells (**Fig. 4**). Together, these lines of evidence indicate that CD11b regulates the Mincle pathway specifically during mycobacterial infection.

3.3. Hyperinflammatory immune response of CD11b$^{-/-}$ mice following TDM stimulation

To examine the inhibitory effect of CD11b on Mincle signaling under physiological conditions, WT and CD11b$^{-/-}$ mice were challenged with TDM to induce a lung granuloma that mimics mycobacterial infection. Intravenous injection of TDM induced granuloma

formation in both WT and CD11b$^{-/-}$ mice, but TDM induced the formation of more severe granulomas in the lungs of the *CD11b*-deficient mice than in the lungs of the WT mice. The relative granuloma area and the lung weight index (LWI), which indicate the severity of the inflammation, were higher in the lungs of CD11b$^{-/-}$ mice than in the lungs of the WT control group (**Fig. 5a, b**). The numbers of recruited neutrophils and monocytes were significantly elevated in the lungs of CD11b$^{-/-}$ mice, in concert with a slight increase in T and B cells compared with the WT mice (**Fig. 5c**). Reflecting the hyperinflammatory conditions in the TDM-stimulated CD11b$^{-/-}$ mice, higher RNA and protein levels of proinflammatory cytokines such as TNF-α and IL-6 were detected in lung homogenates from CD11b$^{-/-}$ mice (**Fig. 5d** and **Fig. 6**). In addition, qRT-PCR analysis revealed a similar upregulation of inflammatory cytokines (*Il1a* and *Il12a*), chemokines (*Ccl2*, *Cxcl2*, and *Cxcl10*), and signaling molecules (*Nos2* and *Mmp3*) in the lungs of CD11b-deficient mice (**Fig. 6**).

To confirm the effect of CD11b on TDM-induced granulomatous tissue formation, the inflammatory activity of TDM was assessed in WT and CD11b$^{-/-}$ mice using an air pouch model[24]. Similar to the results obtained with intravenous injection of TDM, we observed significantly increased levels of leukocytes and inflammatory cytokines (TNF-α and IL-6) in the TDM-stimulated air pouches in CD11b$^{-/-}$ mice compared with WT mice (**Fig. 5e-f**). Taken together, these results indicate that TDM challenge leads to exaggerated inflammatory responses in CD11b$^{-/-}$ mice, suggesting that CD11b is required for the downregulation of inflammation and granuloma formation induced by Mincle activation.

3.4. Impaired adhesion but increased TDM signaling in CD11b$^{-/-}$ neutrophils

To determine whether CD11b can inhibit Mincle signaling in other cell types, the anti-TDM response was examined in neutrophils derived from WT and CD11b$^{-/-}$ mice. As described previously[12], TDM stimulation increased the surface expression of CD11b and its binding partner CD18 in the WT bone marrow (BM)-derived neutrophils. On the other hand, CD11b-deficient BM neutrophils exhibited much less CD18 surface expression than WT BM neutrophils, and this expression did not increase following TDM treatment (**Fig. 7a**). In accordance with the increased CD11b/CD18 surface expression, WT BM-derived neutrophils showed increased adhesion to a TDM-coated surface, while no apparent cell adhesion was observed from the CD11b$^{-/-}$ BM-derived neutrophils (**Fig. 7b**). Despite the reduced levels of adhesion, the secretion of TNF-α and IL-6 was higher in CD11b$^{-/-}$ BM neutrophils than in WT BM neutrophils, and cytokine production was further enhanced in the CD11b$^{-/-}$ neutrophils by IFN-γ treatment (**Fig. 7c**). To determine whether the altered cytokine production may have resulted from an effect of CD11b deficiency on neutrophil survival, apoptosis induced by TDM treatment was evaluated in WT and CD11b$^{-/-}$ neutrophils. TDM stimulation increased neutrophil apoptosis in WT and CD11b$^{-/-}$ BM neutrophils at a similar rate (**Fig. 8a**). Taken together, these findings demonstrate that CD11b is required for cell adhesion and inhibition of cytokine production upon TDM stimulation but does not impact TDM-induced apoptosis in neutrophils.

Although CD11b has been shown to be required for the induction of MyD88-dependent TLR signaling in DCs[21], WT and CD11b$^{-/-}$ DCs stimulated with a synthetic analog of TDM, trehalose-6,6-dibehenate (TDB), showed no apparent difference in the secretion of the

inflammatory cytokines TNF-α and IL-6 (**Fig. 8b**). Therefore, CD11b appears to play an inhibitory role in Mincle signaling in macrophages and neutrophils specifically.

3.5. CD11b interacts with Mincle specifically upon TDM treatment

As Mincle signaling is negatively regulated by CD11b following TDM stimulation, we next examined whether CD11b directly interacts with Mincle and/or its downstream adaptor proteins and regulators. Because Syk binds FcRγ, which is the adaptor molecule for Mincle[25], we first examined the association between Mincle and Syk via a proximal ligation assay (PLA) in immortalized BMMs (iBMMs) transiently transfected with epitope-tagged Mincle and Syk. A PLA with antibodies recognizing the specific epitopes tagged to Mincle and Syk revealed a number of strong signals regardless of TDM treatment (**Fig. 9a**). We next examined the interaction of CD11b with Mincle. Although there was no PLA signal between Mincle and CD11b under resting conditions, the number of interaction signals dramatically increased following TDM stimulation. In addition, no binding between CD11b and Mincle was observed following LPS stimulation, demonstrating that TDM specifically induced their interaction (**Fig. 9b**).

Stimulation of integrins by fibrinogen is known to initiate a strong outside-in activation signal, including the binding of talin to integrin[26]. We asked whether the TDM-dependent binding of Mincle to CD11b also activates CD11b in macrophages. To this end, the interaction between the CD11b/CD18 heterodimer and talin on iBMMs after treatment with fibrinogen or TDM was examined by PLA. Under basal conditions, no interaction between CD11b/CD18 and talin was observed; however, TDM treatment induced strong binding,

similar to the effects of fibrinogen treatment on CD11b/CD18 and talin (**Fig. 9c**). Intriguingly, these interactions required functional CD11b/CD18 heterodimers, as CD11b deficiency disrupted the interaction between CD18 and talin upon stimulation with TDM or fibrinogen. These results indicate that Mincle signaling triggers CD11b/CD18 integrin activation in macrophages; the activated integrin receptors then downregulate Mincle signaling through a direct interaction.

3.6. Activated CD11b attenuates Mincle signaling via Lyn kinase

To understand the regulatory role of CD11b in Mincle signaling, BMMs were treated with inhibitors of various signaling pathways and TDM-induced secretion of IL-6 was examined. Inhibitors of Syk, Erk1/2 (U0126), and IKK (parthenolide) abolished TDM-induced IL-6 cytokine production completely, demonstrating their involvement in Mincle-dependent IL-6 production. Interestingly, treatment with Src family tyrosine kinase (SFK) inhibitors (PP1 and PP2) actually increased IL-6 production after TDM stimulation, consistent with the upregulation observed in TDM-stimulated CD11b-deficient macrophages (**Fig. 10a**). Mincle-dependent Syk and Erk1/2 phosphorylation was also highly enhanced in PP1-treated macrophages upon TDM stimulation (**Fig. 10b**). Similarly, PP1 treatment resulted in increased IL-6 production in neutrophils, but impaired cell adhesion, as described previously[12] (**Fig. 10c, d**). These results indicate that both Mincle-dependent cell adhesion and cytokine production are regulated by SFKs. To identify which SFKs were targeted by PP1 under the conditions described above, the expression of various SFKs was examined in TDM-treated WT and $CD11b^{-/-}$ macrophages by qRT-PCR. Among the nine SFKs examined, *Fgr*, *Hck*, and

Lyn were induced in WT macrophages by TDM treatment, and *Lyn* was strongly increased in CD11b$^{-/-}$ macrophages (**Fig. 10e**). Furthermore, treatment of neutrophils with a Lyn-specific inhibitor increased their IL-6 production significantly, without impairing cell adhesion (**Fig. 10c, d**). These results suggest that Lyn kinase is the SFK primarily mediating the inhibitory effect of CD11b signaling against Mincle-dependent proinflammatory cytokine production.

To confirm the role of *Lyn* in Mincle-mediated signaling, *Lyn* was knocked out in iBMMs using the Cas9/CRISPR system (**Fig. 11a**). Compared with WT iBMMs, Lyn$^{-/-}$ iBMMs showed enhanced Syk and Erk1/2 phosphorylation and stronger induction of proinflammatory genes, including *Tnf*, *Il6*, *Ccl2*, *Cxcl2*, and *Nos2*, upon TDM stimulation (**Fig. 11b and Fig. 12**). Together, these results suggest that CD11b regulates the Mincle pathway through the Lyn kinase.

3.7. TDM-dependent binding of Lyn with CD11b, Mincle, and SHP1

Next, the association between Lyn and CD11b in macrophages was examined. Although no interaction was observed between CD11b and Lyn under basal conditions, TDM stimulation strongly induced this interaction (**Fig. 13 a**). Consistent with the TDM-dependent binding of Mincle to CD11b, Lyn and Syk also exhibited TDM-dependent binding to CD11b (**Fig. 13a**). Therefore, TDM stimulation appears to induce the formation of a receptor complex that includes Mincle, CD11b, and their interacting adaptors and kinases.

Previous studies revealed that the repressive role of the tyrosine kinase Lyn mainly relies on the recruitment of inhibitory phosphatases such as SH2 domain-containing phosphatase 1 (SHP1), SHP2, and SH2 domain-containing 5'-inositol phosphatase (SHIP1)[27]. PLAs were

performed before and after TDM treatment to identify the specific interacting phosphatase(s) of Lyn in response to TDM stimulation. Among the three phosphatases tested, only SHP1 interacted with Lyn and Syk specifically upon TDM treatment (**Fig. 13b, c**). These interactions appeared to be dependent on CD11b, in that no such interaction was detected in CD11b-deficient cells. In addition, the TDM-dependent Syk-SHP1 interaction was defective in $Lyn^{-/-}$ iBMMs. These results indicate that activated Mincle induces formation of an adaptor complex with CD11b signaling molecules.

We next tested whether the phosphatase activity of SHP1 is required for the downregulation of Mincle signaling, particularly the Syk phosphorylation. To this end, the Mincle/CD11b receptor complex was reconstituted in human embryonic kidney 293 (HEK293) cells by co-transfecting expression constructs for Mincle, FcRγ, Syk, and either WT or dominant-negative SHP1 (D419A and C453S). In the reconstituted cells, TDM treatment induced Syk phosphorylation, which was diminished significantly by the addition of functional SHP1 (**Fig. 13d**). The dominant-negative forms of SHP1, however, failed to dephosphorylate Syk. Therefore, recruitment of SHP1 by activated CD11b dephosphorylates Syk, resulting in the inhibition of Mincle signaling.

3.8. SIRPα is critical for the SHP1 recruitment

SHP1 phosphatase recruitment normally requires immunoreceptor tyrosine-based inhibitory motif (ITIM)-containing receptors to serve as docking sites. The two ITIM-containing receptors Pirb and SIRPα have been studied extensively in association with SHP1[28, 29]. To determine which receptor can associate with SHP1 and Lyn upon TDM

stimulation, a PLA assay was performed. Pirb exhibited strong binding with CD11b, Syk, Lyn, and SHP1 independently of TDM treatment (**Fig. 14 a**); however, no interaction signal was observed for Pirb with Mincle even in the presence of TDM stimulation. These results indicate that Pirb may interact with SHP1 but that this interaction is not related to the Mincle signaling pathway. On the other hand, although SIRPα did not interact with any of the Mincle/CD11b receptor complex components tested under resting conditions, this receptor produced strong PLA signals with CD11b, Syk, Lyn, SHP1, and Mincle upon TDM stimulation (**Fig. 14b**). In addition, binding of SIRPα to the CD11b/Mincle complex was nearly completely disrupted in $Lyn^{-/-}$ and $Syk^{-/-}$ iBMMs **(Fig. 15)**. Therefore, SIRPα appears to be a member of the Mincle/CD11b receptor complex.

To investigate the requirement of SIRPα for the regulation of Mincle signaling, SIRPα-deficient iBMM cell lines were generated and evaluated for their response to TDM challenge (**Fig. 16a**). Phosphorylation of Syk and Erk1/2 in response to TDM stimulation was preserved in $SIRP\alpha^{-/-}$ cells (**Fig. 16b**). In addition, $SIRP\alpha^{-/-}$ cells secreted more TNF-α and IL-6 and had stronger induction of proinflammatory genes (*Tnf*, *Il6*, *Il1α, Ccl2*, and *Il12b*) than WT cells (**Fig. 16c and Fig. 12**). Furthermore, the Lyn-SHP1 interaction was also disrupted in $SIRP\alpha^{-/-}$ iBMMs (**Fig. 6b**), suggesting that SIRPα was required for CD11b-mediated negative regulation of Mincle signaling.

To examine the physiological relevance of the iBMM-based analysis system, rescue experiments were performed for CD11b and Syk in iBMM cell lines with deletions of the corresponding genes. CD11b-deficient iBMMs showed enhanced Mincle-dependent IL-6 production, as did the $CD11b^{-/-}$ BMMs, while transfection with Flag-tagged CD11b reduced

the Mincle signal. In addition, Mincle signaling was almost completely abrogated in the Syk-deficient iBMMs, but transfection with Flag-tagged Syk rescued Mincle-dependent IL-6 production in those cells **(Fig. 17)**.

3.9. CD11b initiates the formation of an inhibitory complex to bind Mincle

To confirm the physical interaction between CD11b and Mincle, a co-immunoprecipitation assay was performed using iBMMs expressing an epitope-tagged Mincle. Immunoprecipitation of Mincle did not pull down CD11b in the absence of TDM treatment. However, the amount of CD11b, Syk, and SHP1 that co-immunoprecipitated with Mincle gradually increased after TDM stimulation (**Fig. 18a**). These interactions appear specific to TDM stimulation, as no such binding was observed when LPS was used instead of TDM (**Fig. 18b**). The interactions among the signaling molecules were further validated using endogenous proteins. Pull-down of Lyn in WT macrophages revealed a TDM-dependent complex containing Lyn, CD11b, SHP1, and Syk that was disrupted in CD11b-deficient macrophages (**Fig. 18c,d**). Moreover, immunoprecipitation with an anti-SHP1 antibody also revealed a TDM- and CD11b-dependent interaction among CD11b, Syk, and SHP1 (**Fig. 18e,f**). Taken together with the PLA results, these data confirm the formation of an inhibitory complex that contains Lyn, Syk, and SHP1 and binds CD11b and Mincle.

3.10. The Lyn activator MLR1023 suppresses Mincle signaling

Because Lyn plays a pivotal role in the CD11b-mediated negative regulation of Mincle signaling, the ability of the Lyn kinase activator MLR1023 to enhance anti-Mincle activity was examined. Contrary to the stimulatory effect of PP1 on TDM-induced proinflammatory

cytokine production (**Fig. 10a**), treatment with MLR1023 arrested TDM-induced IL-6 production in WT macrophages and restored the hyperinflammatory response of $CD11b^{-/-}$ macrophages to levels similar to those seen in WT macrophages (**Fig. 19a**). Furthermore, MLR1023 treatment reduced the TDM-dependent phosphorylation of Syk and Erk1/2 in both WT and $CD11b^{-/-}$ BMMs (**Fig. 19b**). These results confirmed the negative regulatory role of Lyn in Mincle signaling.

To examine the physiological relevance of CD11b-mediated inhibition of Mincle-dependent inflammation, the effect of enhanced CD11b signaling on TDM-induced granuloma formation in mice was investigated. The Lyn activator MLR1023 was administered to TDM-challenged mice and the effects on TDM-induced granuloma formation were examined. Compared with the control group, MLR1023-treated mice exhibited less severe TDM-induced lung granulomas and lung swelling (**Fig. 19c, d**). Leukocyte recruitment to the lung (**Fig. 19e**) and TNF-α and IL-6 production (**Fig. 19f**) were also decreased in the MLR1023-treated mice, indicating that MLR1023 suppresses TDM-induced inflammation. Intriguingly, MLR1023 treatment also decreased the TDM-induced granuloma response in $CD11b^{-/-}$ mice **(Fig. 20)**, confirming the epistatic effect of Lyn in the CD11b signaling pathway. Therefore, CD11b signaling plays an important inhibitory role in the regulation of Mincle-dependent inflammatory responses against mycobacterial infection. These data suggest that the Lyn kinase may be an effective target for the treatment of the excessive inflammatory response caused by this infection.

4. Discussion

Mincle plays a central role in the host defense against mycobacterial infection as the major receptor for mycobacterial cell wall component TDM. The activating role of this signaling molecule in the proinflammatory response has been well studied; however, little is known about the mechanism that leads to dampening of this inflammatory signal. In this study, we provide multiple lines of evidence demonstrating that CD11b is the crucial negative regulator of Mincle signaling and therefore plays an important role in Mtb infection.

First of all, our observation that CD11b deficiency resulted in a significantly enhanced Mincle-dependent inflammatory response against TDM and BCG challenge extends the function of CD11b in Mtb infection. Phagocytes from patients with tuberculosis possess augmented CD11b/CD18 expression, which is thought to promote cell adhesion and accumulation at the infection site[30]. During Mtb infection, the immune response is mediated by TLRs, which are activated by various molecular patterns on Mtb[31]. Recent work revealed that CD11b facilitates proteasomal degradation of Myd88 and TRIF upon TLR3, 4, and 9 activation, thereby inhibiting the inflammatory response[14]. Yi Bang also reported that CD11b

downregulates DC-mediated cross-priming through miR-146a[32]. Here, we demonstrated that CD11b interferes with the proinflammatory response induced by the Mtb-specific PAMP TDM and confirmed that live Mtb infection also induces increased cytokine production in CD11b$^{-/-}$ BMMs. Although TLR and Mincle signaling are negatively regulated by CD11b through different mechanisms, these signals converge on nuclear transcription factor-kappaB (NF-κB) and synergistically enhance the inflammatory response toward Mtb infection[33, 34]. Altogether, CD11b appears to play a broad role in the negative regulation of the proinflammatory response toward PAMPs expressed by Mtb.

Moreover, CD11b may be involved in inflammatory responses toward Mtb infection via another Mincle ligand. During the late phase of Mtb infection, infected macrophages are cleared by apoptosis, necrosis, and autophagy[35]. Necrotic cell death results in the release of spliceosome-associated protein 130 (SAP130), a soluble component of the U2 small nuclear ribo-nucleoprotein-associated protein that is normally found in the nucleus[36]. Yamasaki et al. reported that ligation of SAP130 to Mincle on macrophages also elicits proinflammatory responses through FcRγ and Card9, similar to the effects of TDM stimulation[25]. Hence, these findings indicate that CD11b may further regulate the immune response during the late stage of Mtb infection through SAP130-mediated Mincle signaling.

Secondly, our results indicate that negative regulation of Mincle signaling by CD11b occurs via the Lyn kinase. As an SFK, Lyn plays both positive and negative roles in modulating immune function and is also associated with integrin-mediated cellular homeostasis[37]. Lyn provides a positive signal via phosphorylation of ITAM-carrying proteins, such as FcRγ, to recruit Syk and activate Syk-mediated signaling[38]. Conversely, Lyn can downregulate signaling via direct interactions with a target protein like interferon regulatory factor (IRF) 5. Lyn ultimately inhibits IRF5 ubiquitination and phosphorylation, impairing the IRF5-mediated TLR-Myd88 signal[39]. Meanwhile, the main negative regulatory role of Lyn is dependent on the recruitment of phosphatases such as SHP1, SHP2, and SHIP1, which target proteins through ITIM domain-carrying receptors such as SIRPα and Pirb. Here, we found that Lyn interacts with CD11b in a Mincle signaling-dependent manner. Following inhibition of Lyn with PP1 in BMMs or deletion of Lyn in iBMMs, we observed a hyper-response toward TDM stimulation similar to that observed in $CD11b^{-/-}$ cells following TDM stimulation. The negative regulatory role of Lyn has been thoroughly investigated within the context of BCR signaling and integrin-mediated adhesion. Recent work defined CD11b as the major modulator in the formation of the inhibitory complex Lyn-CD22-SHP1, which restrains BCR signals[16]. In addition, $Lyn^{-/-}$ macrophages

display decreased activation of SIRPα, Pirb, and SHP1 upon growth factor stimulation, suggesting that Lyn, SIRPα/Pirb, and SHP1 may function together to exert negative regulatory effects in response to growth factors[40]. Similar to these findings, we found that Lyn dephosphorylates Syk, a target previously known to be positively regulated by Lyn. This dephosphorylation was mediated by Lyn's recruitment of SHP1 to the docking protein SIRPα in a CD11b-dependent manner.

Treatment of cells with PP1 during TDM stimulation revealed a broad role for SKFs in Mincle signaling. Integrin activation can be more easily studied in neutrophils than in macrophages, as robust functional readouts exist for these cells[41]. Upon integrin activation, neutrophils show greatly enhanced adhesion. TDM stimulation facilitated adhesion in neutrophils, which was abrogated by PP1 treatment or CD11b deficiency, but not by inhibition of Lyn. These results suggest that CD11b plays a major role in TDM-induced neutrophil adhesion, while SFKs besides Lyn could positively modulate this process. On the other hand, utilizing a Lyn-specific inhibitor led to enhanced cytokine production in neutrophils, with no influence on cell adhesion. These findings are consistent with our predicted model, in which Lyn is critical for the formation of an inhibitory complex that is

dependent on signals transduced by activated CD11b, but does not affect CD11b-mediated adhesion induced by TDM.

In addition, treatment with the Lyn activator MLR1023 inhibited Mincle signaling both *in vitro* and *in vivo*. MLR1023 is a selective Lyn activator and a potential insulin sensitizer that was developed as a candidate therapeutic drug for type II diabetes[42]. Interestingly, enhanced Mincle expression was detected in obesity-induced adipose tissue fibrosis, suggesting that augmented Mincle signaling may contribute to adipose tissue fibrosis formation and thereby promote obesity[43]. Fibrosis is a similar process to granuloma formation and involves the accumulation of activated macrophages that highly express CD11b[44, 45]. In our granuloma model, treatment of TDM-challenged mice with MLR1023 decreased Mincle signaling and inhibited granuloma formation. Therefore, MLR1023 treatment of obese mice may also decrease adipose fibrosis formation by inhibiting Mincle signaling. Recently, Lee and colleagues found that enhanced Mincle signaling is strongly correlated with uveitis, an autoimmune disease of the eye[46]. Thus, further studies might be warranted to determine whether treatment with MLR1023 could inhibit Mincle signaling in these Mincle-related diseases.

Finally, regulation of CD11b in TDM-Mincle signaling specifically affects macrophages and neutrophils, but not DCs. Although CD11b is as highly expressed in DCs as in macrophages[47], its function might vary in different cell

types, even in response to the same stimulation. For example, in the context of LPS stimulation, CD11b exerts a negative role in macrophages by facilitating the degradation of Myd88 and TRIF[14], but positively influences LPS signaling in DCs[21]. Meanwhile, SHP1 has also been reported to form an inhibitory axis following activation by Mincle signaling in DCs; this results in reduced adaptive immunity to *Leishmania major* infection[48]. However, in that paper, TDB was not the inducer of the Mincle-SHP1 interaction in DCs. Therefore, the Lyn-SIRPα-SHP1 inhibitory complex may be formed specifically in response to Mincle signaling in macrophages and neutrophils.

Similarly, Lyn and SIRPα were observed to have opposing effects in deficient iBMMs, which might be explained by the multiple biological functions of Lyn and SIRPα. Lyn is particularly well-known as a dual functional regulator in macrophages, where it negatively regulates signaling induced by growth factors and integrin activation[37]. Some studies have also implicated Lyn activation particularly in signaling through the IL-3 and IL-6 receptors[49]. Meanwhile, SIRPα can bind to and be activated by the transmembrane protein CD47, which is expressed on immortalized cell lines like the iBMMs that were used in this study[50]. SIRPα-CD47 binding can induce a variety of signaling pathways that result in the inhibition of phagocytosis[51]. Also, SIRPα expressed on macrophages can

attenuate mitogen-activated protein kinase (MAPK) signaling and NF-κB activation in response to LPS treatment through an association with SHP2[52]. Considering that both Lyn and SIRPα could specifically regulate the production of distinct cytokines via divergent pathways, a deficiency in either Lyn or SIRPα may have a distinct influence on the major inhibitory function of CD11b-SHP1 in Mincle signaling.

In conclusion, we demonstrated that activation of CD11b in response to TDM acts as a critical negative regulator of Mincle signaling by promoting formation of a Lyn-SIRPα-SHP1 complex that dephosphorylates Syk. CD11b deficiency led to a hyper-response against TDM challenge, while Lyn activation by MLR1023 exerted the opposite effect and impaired the TDM-induced inflammatory response. Our results provide insight into the mechanisms involved in fine-tuning Mincle signaling during the inflammatory response and suggest Lyn as a potential target for modulation of the immune response during Mtb infection.

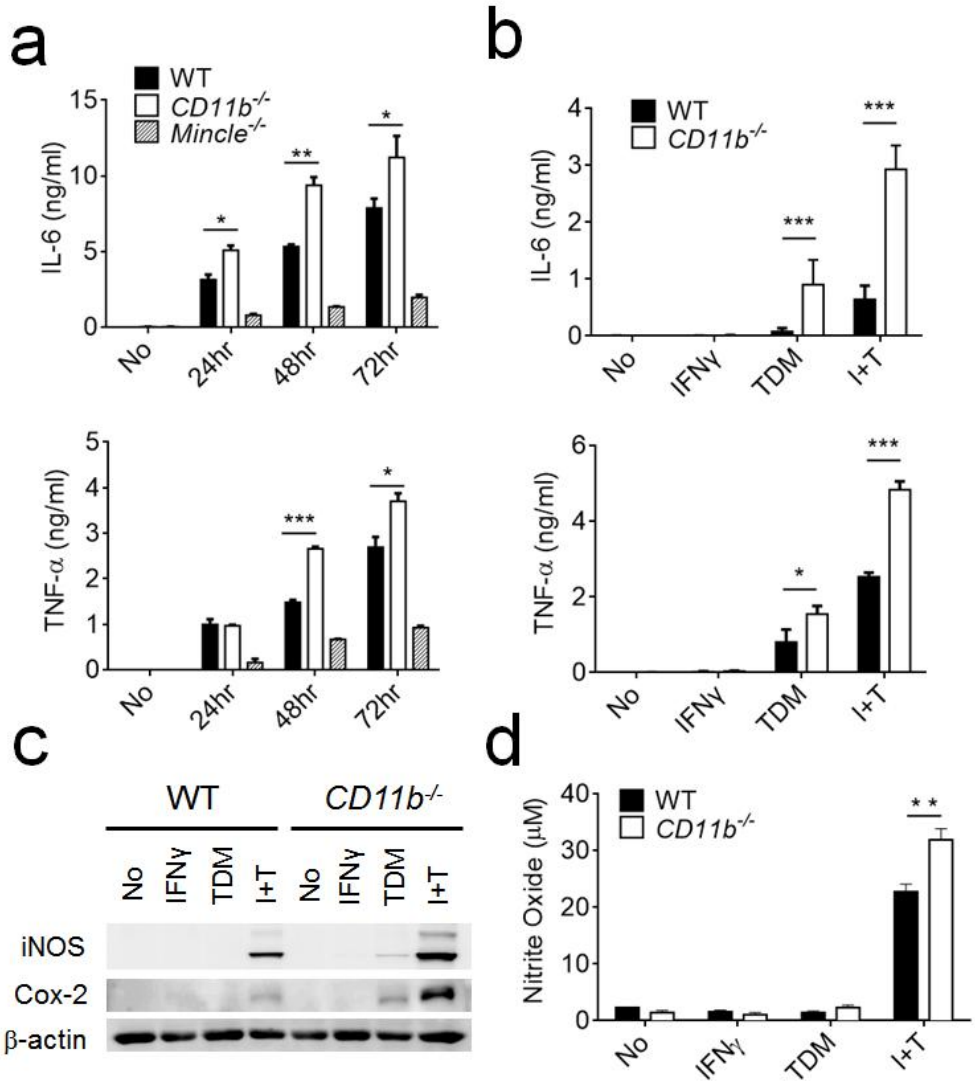

Figure 1. ***CD11b*** **deficiency enhances the macrophage response to BCG infection and TDM stimulation.**

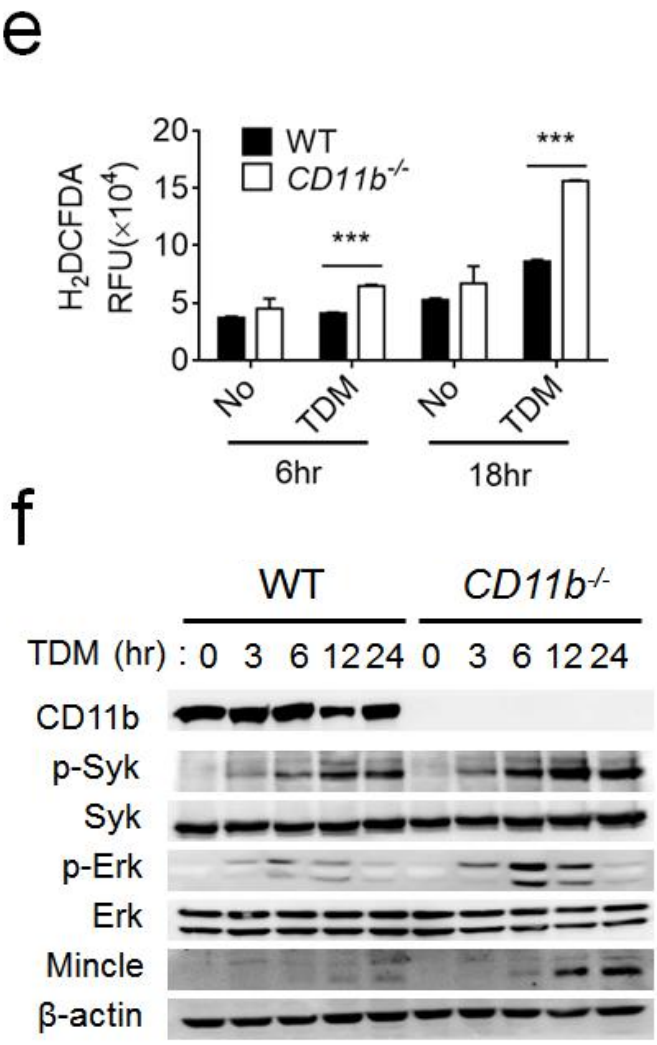

- continued Figure 1.

Figure 1. *CD11b* deficiency enhances the macrophage response to BCG infection and TDM stimulation.

(**a**) BMMs from WT, *CD11b*$^{-/-}$, and *Mincle*$^{-/-}$ mice were infected with BCG at a MOI of 5, and the cell culture supernatants were collected at the indicated time points. Secreted cytokines (IL-6 and TNF-α) were assayed with ELISA. (**b-d**) WT and *CD11b*$^{-/-}$ BMMs were stimulated with 10 ng/ml IFNγ or 50 μg/ml TDM or co-stimulated with TDM and IFNγ (I+T) for 24 h. (**b**) IL-6 and TNF-α cytokine levels from culture media were determined by ELISA. (**c**) Expression levels of iNOS, Cox-2, and total protein were determined by western blot. (**d**) NO generated in the cell supernatant was measured using the Griess reagent. (**e**) Induction of ROS was determined using the H_2DCFDA assay 6 and 18 h after stimulation with 50 μg/ml TDM. (**f**) Phosphorylation of Syk and Erk kinases in WT and *CD11b*$^{-/-}$ BMMs was analyzed by immunoblot at the indicated times. β-actin protein level was used as loading control in western blot assay. Data are representative of at least three independent experiments. **P*<0.05, ***P*<0.01, ****P*<0.0001 (two-tailed unpaired Student's *t*-test).

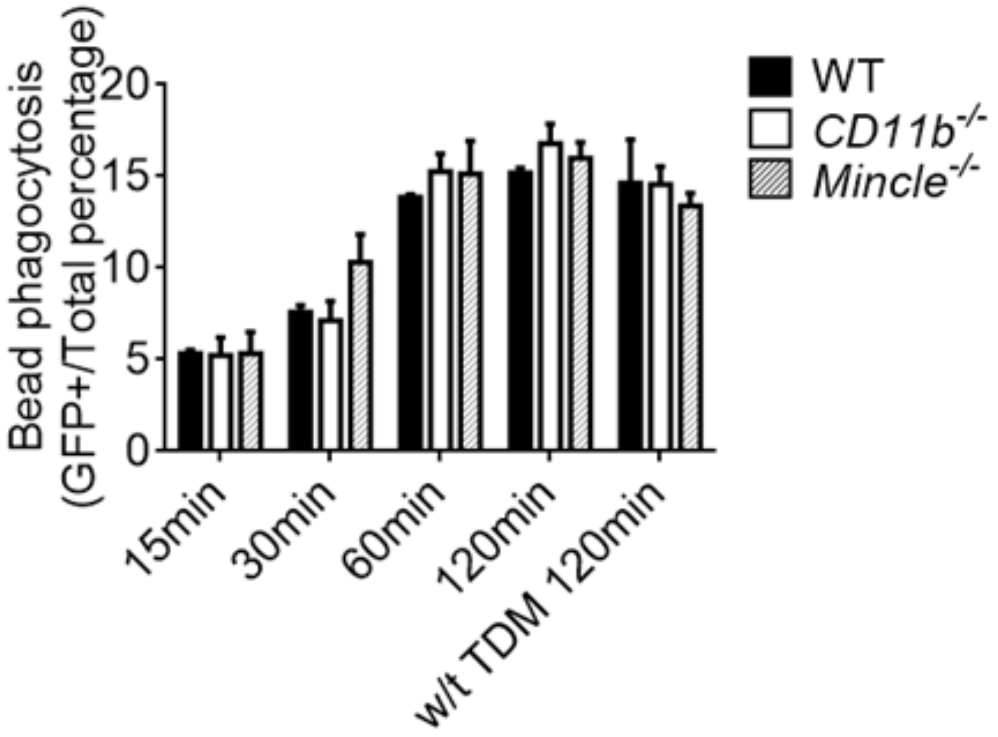

Figure 2. Phagocytosis of GFP- and TDM-labelled beads was not altered in BMMs from WT, *CD11b*$^{-/-}$, or *Mincle*$^{-/-}$ mice.

Figure 2. Phagocytosis of GFP- and TDM-labelled beads was not altered in BMMs from WT, *CD11b*$^{-/-}$, or *Mincle*$^{-/-}$ mice.

Macrophages from WT, *CD11b*$^{-/-}$, and *Mincle*$^{-/-}$ mice were plated and incubated overnight, and GFP-labelled or TDM-coated latex beads were added to the culture. Cells were collected at the indicated times, and internalization of the beads was analyzed with flow cytometry. Data are representative of three independent experiments.

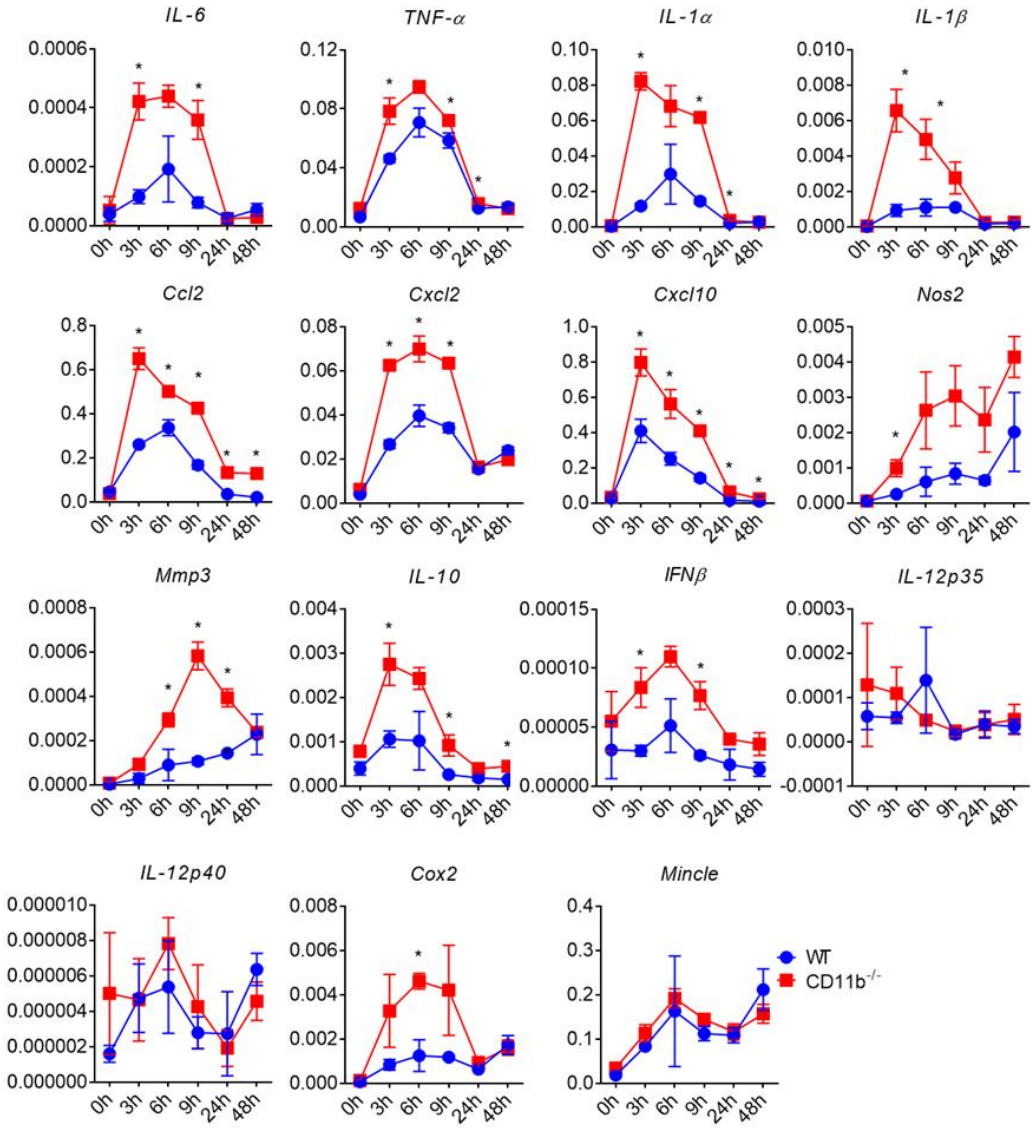

Figure 3. Enhanced proinflammatory gene expression in *CD11b* $^{-/-}$ BMM upon TDM stimulation.

Figure 3. Enhanced proinflammatory gene expression in *CD11b* $^{-/-}$ BMM upon TDM stimulation.

Relative mRNA expression of proinflammatory genes was quantified in WT and *CD11b*$^{-/-}$ BMM treated with TDM (50 mg/ml) for the indicated times. Data are representative of three independent experiments. **P*<0.05, ***P*<0.01, ****P*<0.0001 (two-tailed unpaired Student's *t*-test).

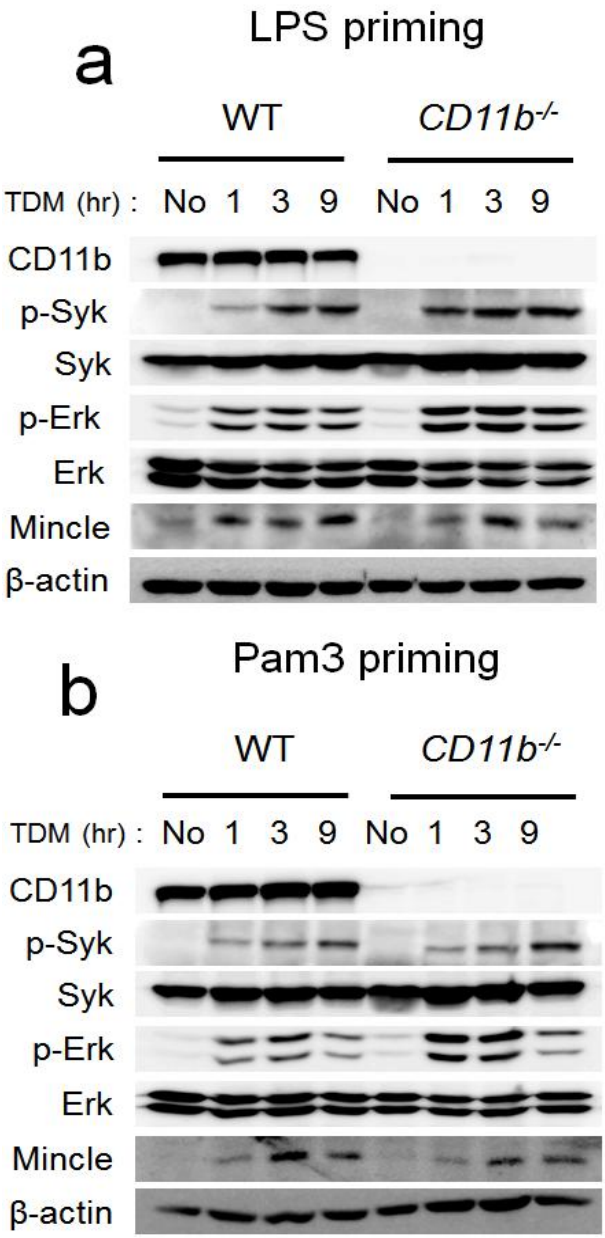

Figure 4. Mincle downstream signal activation in LPS- or Pam3-primed, TDM-simulated WT and *CD11b*$^{-/-}$ macrophages.

Figure 4. Mincle downstream signal activation in LPS- or Pam3-primed, TDM-simulated WT and *CD11b*$^{-/-}$ macrophages.

Macrophages from WT and *CD11b*$^{-/-}$ mice were pretreated with (10 ng/ml) LPS or (100 ng/ml) Pam3 for 3 h and then challenged with TDM for the indicated times. Total protein and phosphorylated Syk and Erk were analyzed by immunoblot assay. β-actin protein expression was used as loading control in western blot assay. Data are representative of two independent experiments.

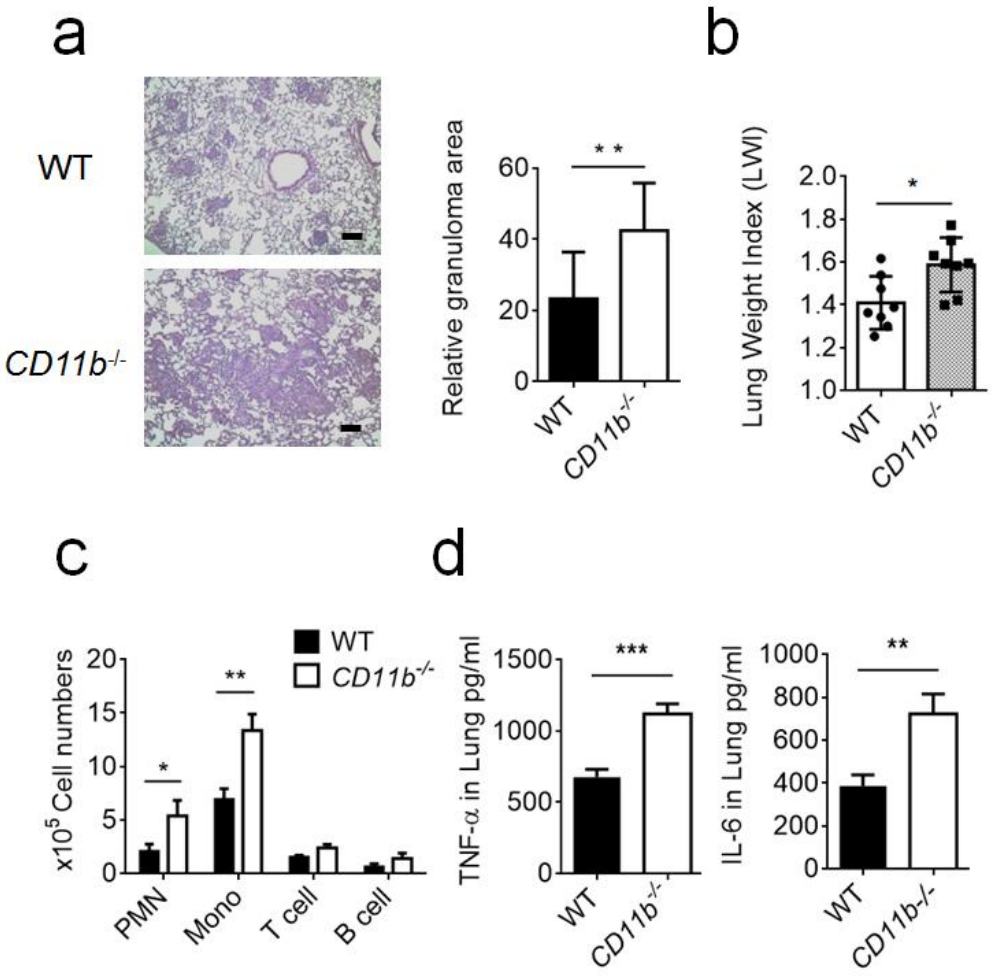

Figure 5. Absence of CD11b leads to more severe granuloma formation and hyperrecruitment of inflammatory cells *in vivo*.

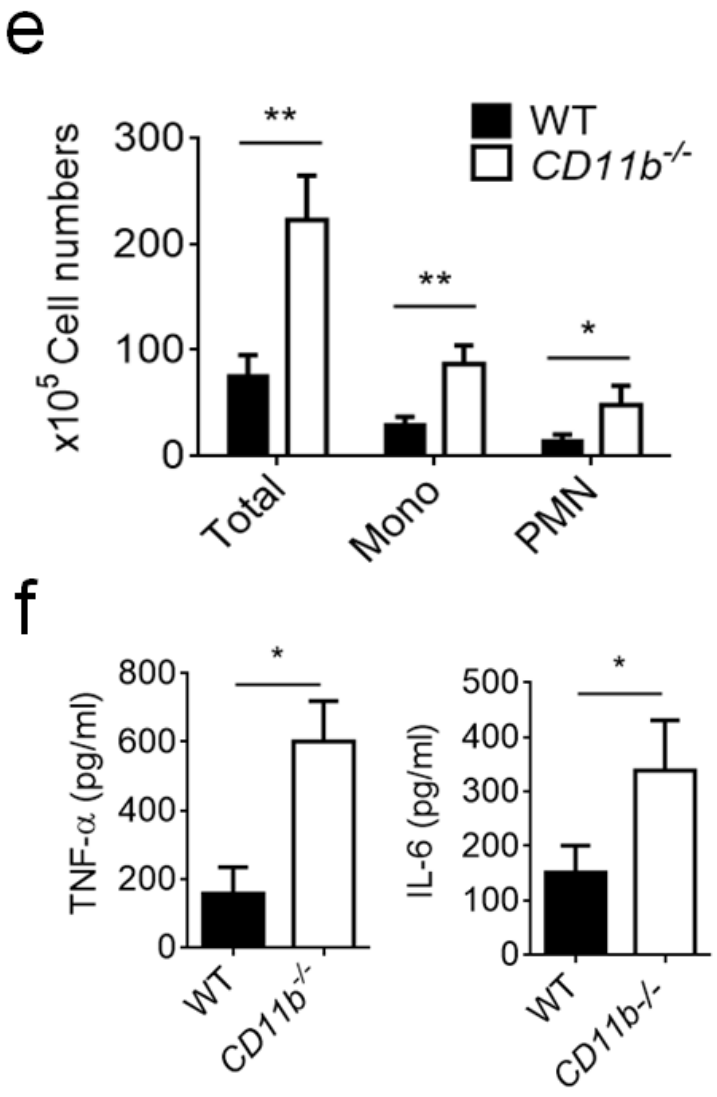

- continued Figure 5.

Figure 5. Absence of CD11b leads to more severe granuloma formation and hyperrecruitment of inflammatory cells *in vivo*.

(**a-d**) WT and *CD11b* KO mice (n=8) were intravenously injected with (3.75 mg/kg) TDM in an oil-in-water emulsion and sacrificed at 7 d post-TDM challenge. (a) Lungs were isolated and stained with hematoxylin and eosin (H&E) for histology analysis after measurement of lung weight for lung weight index (LWI) calculations shown in (**b**). Scale bars, 100 mm. (**c**) Flow cytometry was performed for leukocyte subset analysis with distinct markers for monocytes and macrophages (Mo/Ma, CD11b+ Ly6G-), neutrophils (PMN CD11b+ Ly6G+), T cells (CD3+), and B cells (CD19+). (**d**) The lung homogenates were analyzed by ELISA for IL-6 and TNF-α production. (**e-f**) For the air pouch model, mice (n=8) were dorsolaterally injected with sterile air on day 0 and day 3 followed by injection of 2.5 mg/kg TDM emulsion on day 7. Then on day 8, (**e**)wash fluid from the pouches were assessed by flow cytometry for leukocyte subsets as described above. (**f**)The IL-6 and TNF-α cytokine levels were determined by ELISA. **P*<0.05, ***P*<0.01, ****P*<0.0001 (two-tailed unpaired Student's *t*-test). Data are representative of two independent experiments. (b-f, mean and s.d. of 8 mice per group).

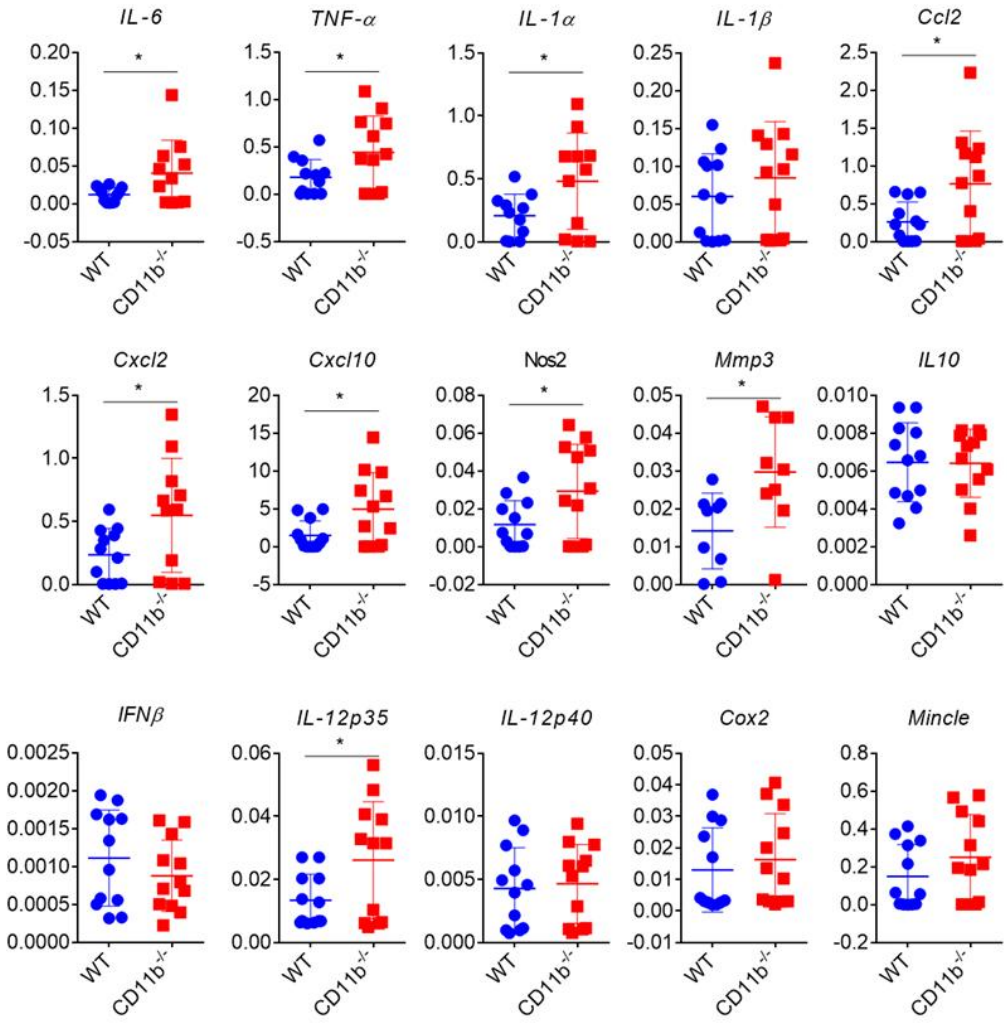

Figure 6. Induction of proinflammatory genes in the lungs of TDM-treated WT and *CD11b*$^{-/-}$ mice.

Figure 6. Induction of proinflammatory genes in the lungs of TDM-treated WT and *CD11b*$^{-/-}$ mice.

Relative mRNA expression of proinflammatory genes in lung homogenates from TDM-challenged WT and *CD11b*$^{-/-}$ mice lung were quantified by qRT-PCR and normalized to *Gapdh*. Data are representative of two independent experiments. *P<0.05 (two-tailed unpaired Student's t-test).

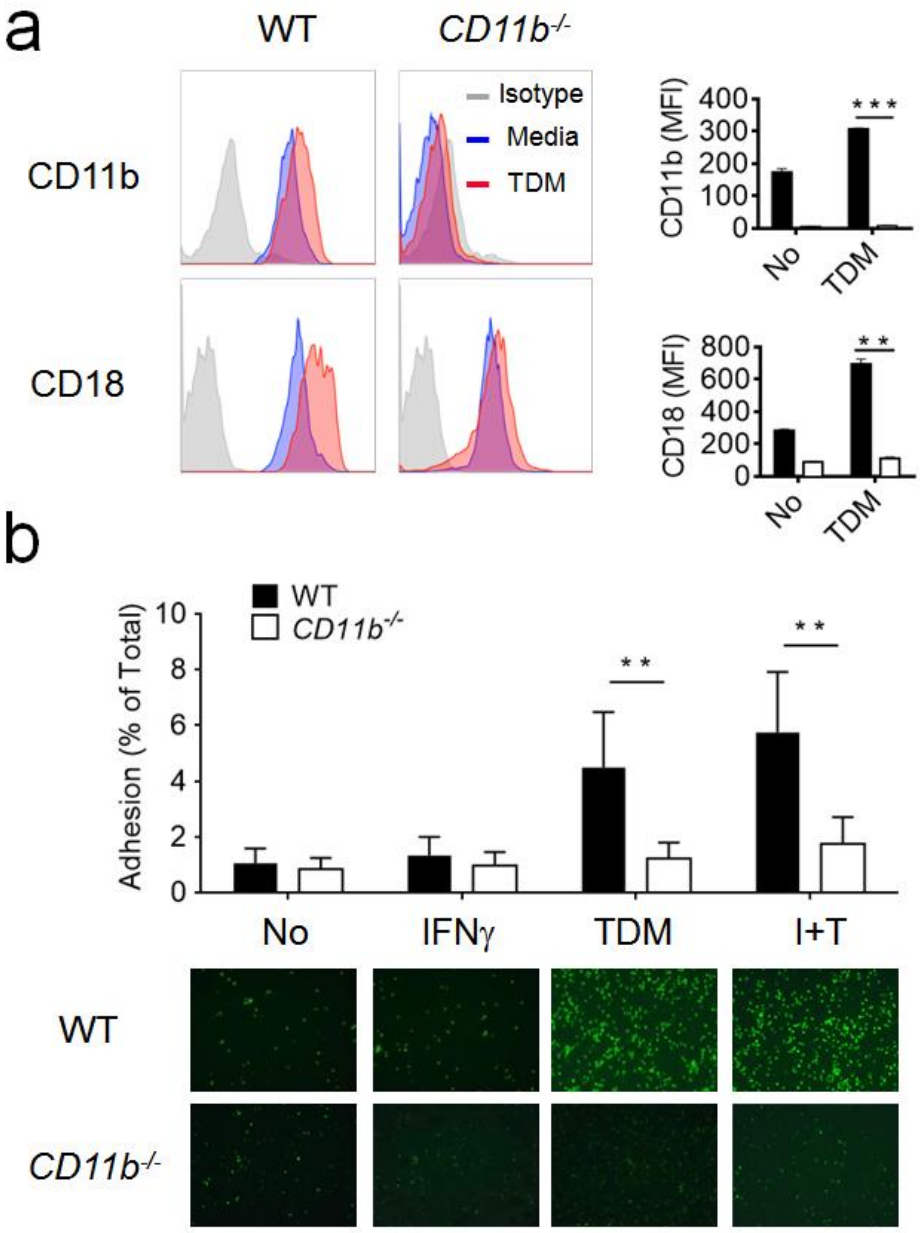

Figure 7. CD11b-deficient neutrophils exhibit impaired adhesion but increased activity upon Mincle activation.

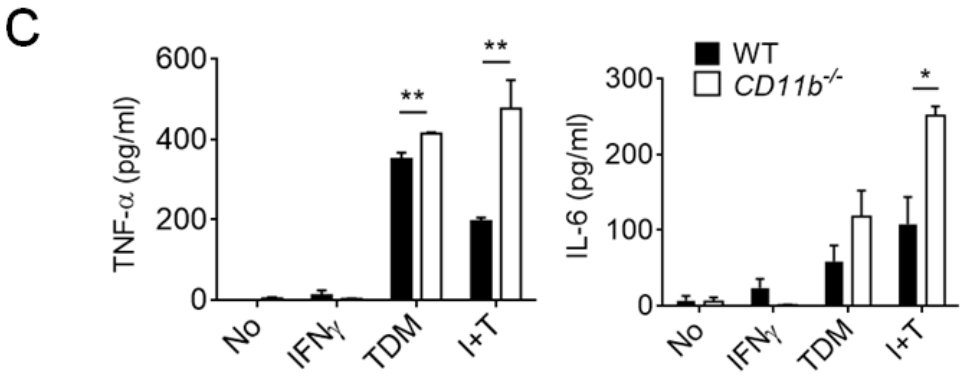

- continued Figure 7.

Figure 7. CD11b-deficient neutrophils exhibit impaired adhesion but increased activity upon Mincle activation.

(**a**) Bone marrow (BM) neutrophils from *CD11b* WT and KO mice were treated with 50 μg/ml TDM, and surface expression of CD11b and CD18 was determined by flow cytometry 24 h after stimulation. (**b**) WT and *CD11b*$^{-/-}$ BM neutrophils were pre-labeled with calcein acetoxymethyl ester 6 h before 50 μg/ml TDM treatment with or without priming with 10 ng/ml IFNγ (I+T). Adhered cells were imaged with fluorescent microscope (bottom panel, 40×). The percentage of adherent cells was determined by comparison of fluorescence measured by a microplate reader at 492 nm before and after washing(**b** top panel). (**c**)IL-6 and TNF-α levels were assayed 24 h after TDM stimulation. Data are representative of three independent experiments. **P*<0.05, ***P*<0.01, ****P*<0.0001 (two-tailed unpaired Student's *t*-test).

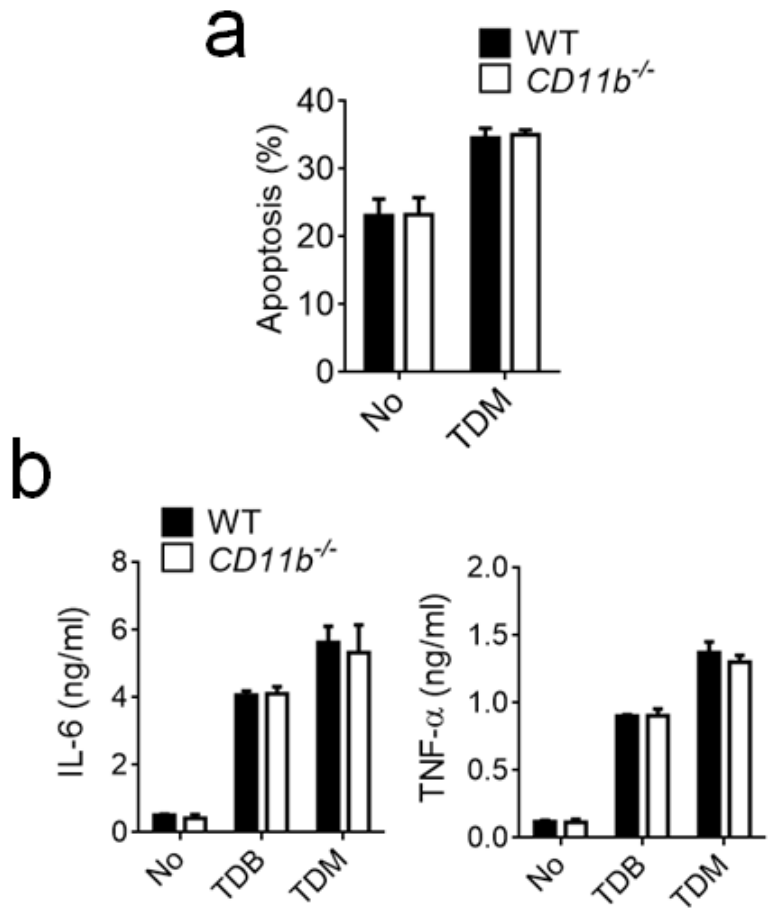

Figure 8. Comparison of neutrophil apoptosis and dendritic cell cytokine production upon activation of Mincle signaling in WT and CD11b$^{-/-}$ cells.

Figure 8. Comparison of neutrophil apoptosis and dendritic cell cytokine production upon activation of Mincle signaling in WT and CD11b$^{-/-}$ cells.

(**a**) WT and CD11b$^{-/-}$ neutrophils were treated with TDM (50 μg/ml) for 24 h. Cells were labeled with Annexin V and propidium iodide (PI) and analyzed by flow cytometry. (**b**) WT and CD11b$^{-/-}$ BMDCs were stimulated with TDM for 24 h, and the levels of TNF-α and IL-6 in the cell culture supernatants were measured by ELISA. Data are representative of three independent experiments. No significant differences were observed ($P>0.05$).

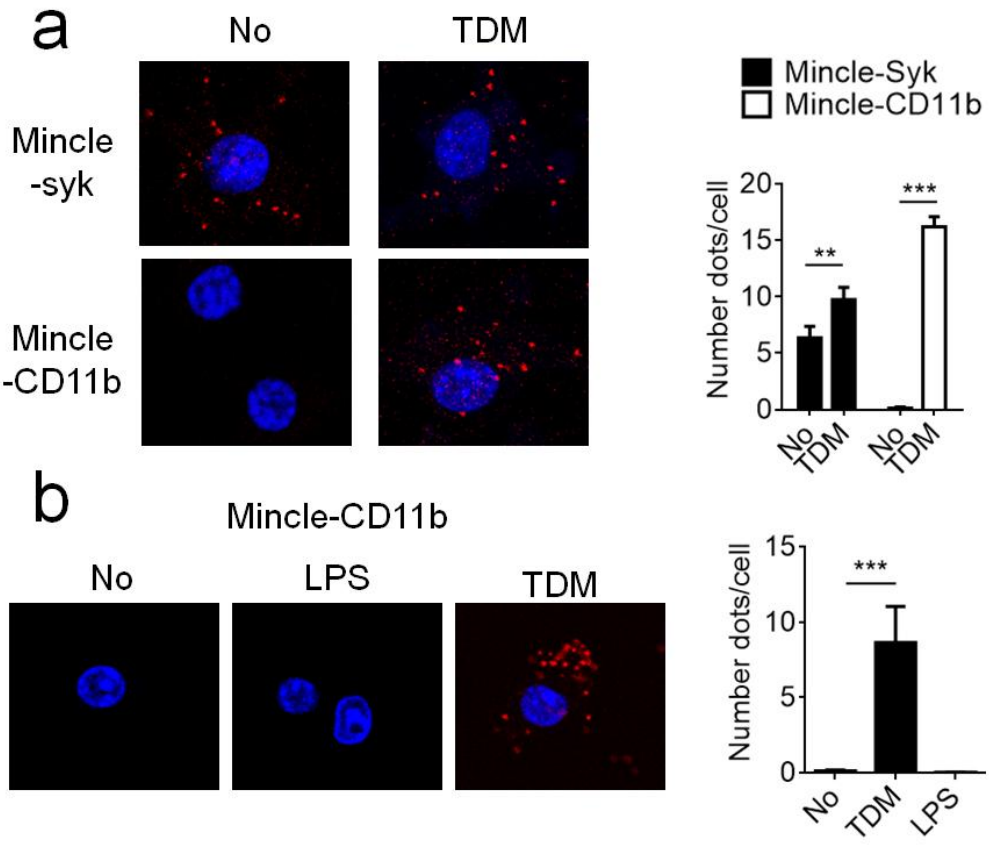

Figure 9. CD11b specifically interacts with Mincle upon TDM treatment

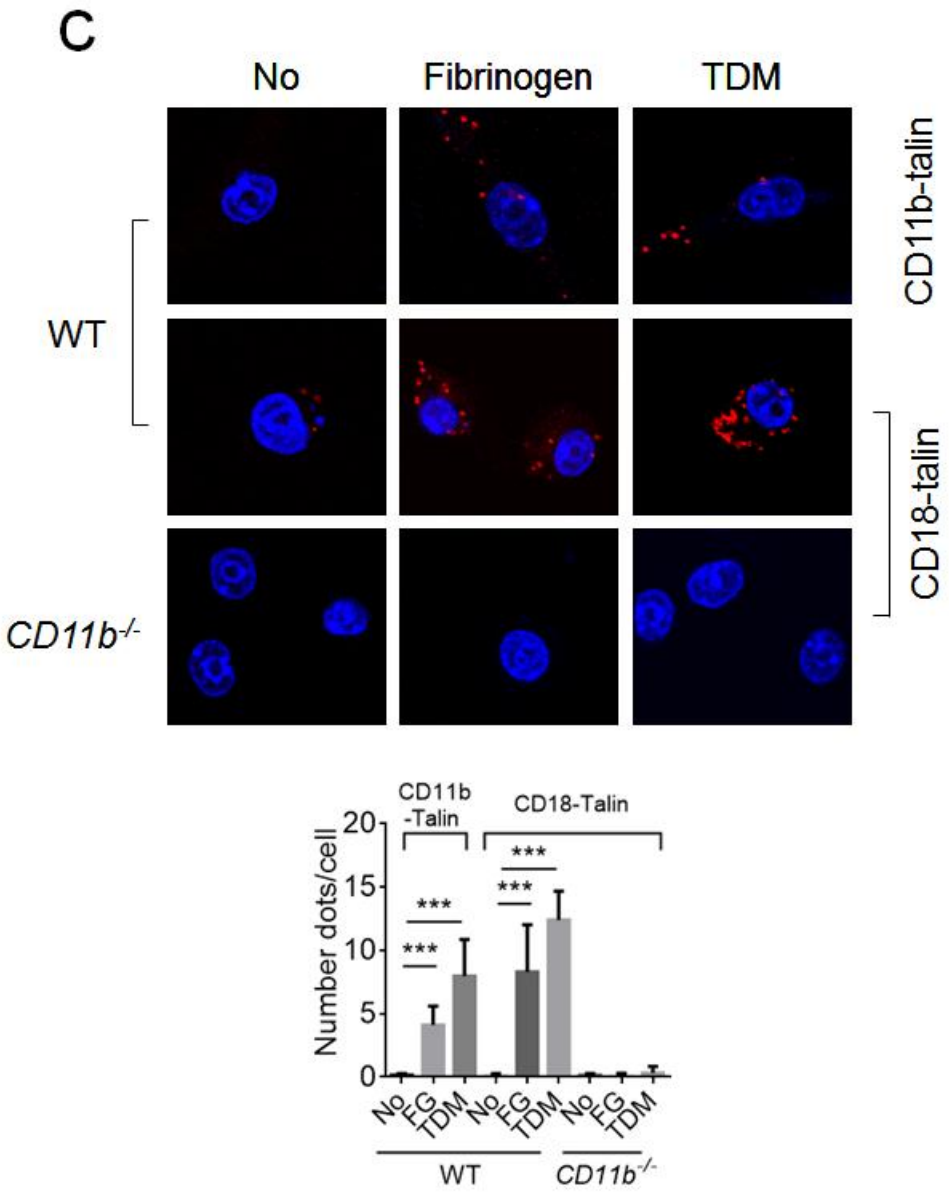

- continued Figure 9.

Figure 9. CD11b specifically interacts with Mincle upon TDM treatment.

iBMM cells were transfected with indicated tagged-plasmids. (**a**) PLA was performed for detection of Mincle-CD11b and Mincle-Syk interactions in iBMMs that were stimulated with TDM for 12 h. (**b**) The Mincle-CD11b interactions following stimulation with TDM (50 μg/ml) for 12 h or LPS (100 ng/ml) for 6 h were compared. (**c**) Interactions of CD11b/CD18 with endogenous talin in WT and $CD11b^{-/-}$ iBMM cells were examined after stimulation with TDM (50 μg/ml) for 24 h or fibrinogen (1 μg/ml) for 30 min. Interactions were visualized as fluorescent spots (red, PLA signal), and nuclei were stained with DAPI (blue). The number of PLA signals was determined for at least 50 cells for each condition. Data are representative of three independent experiments. $^{**}P<0.01$, $^{***}P<0.0001$ (two-tailed unpaired Student's *t*-test).

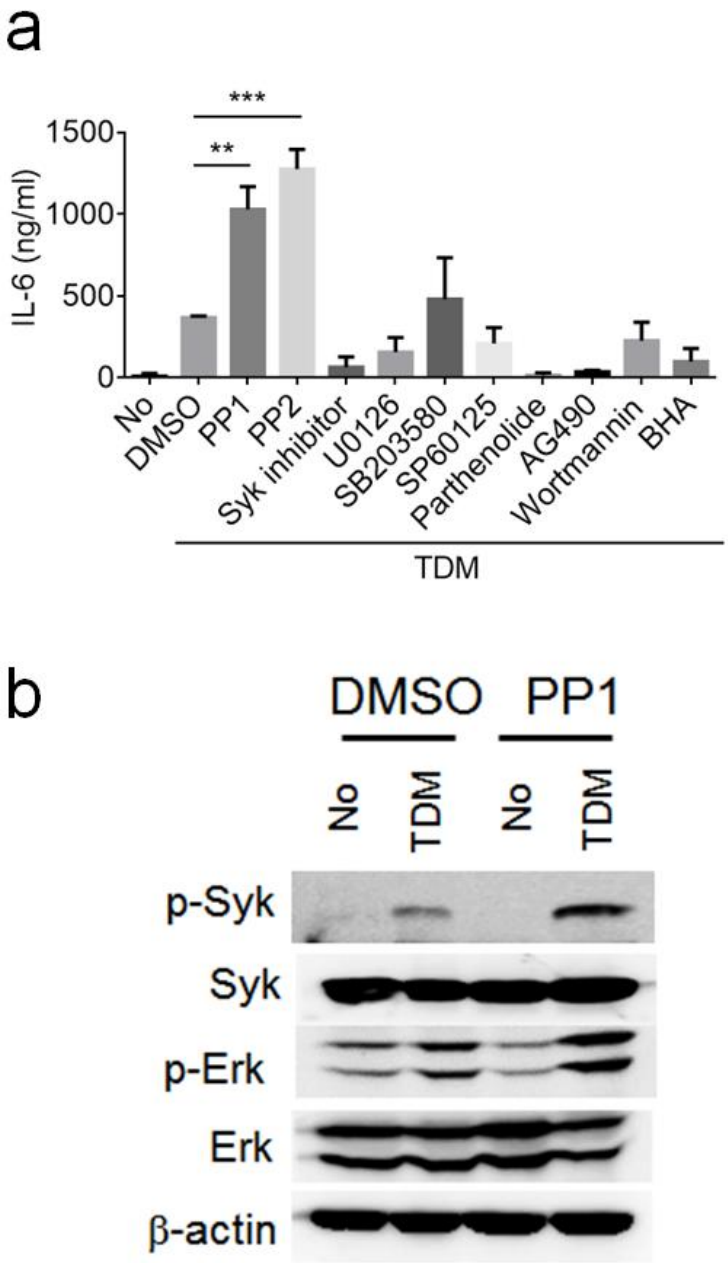

Figure 10. Lyn inhibits Mincle signaling by interfering with Mincle downstream target.

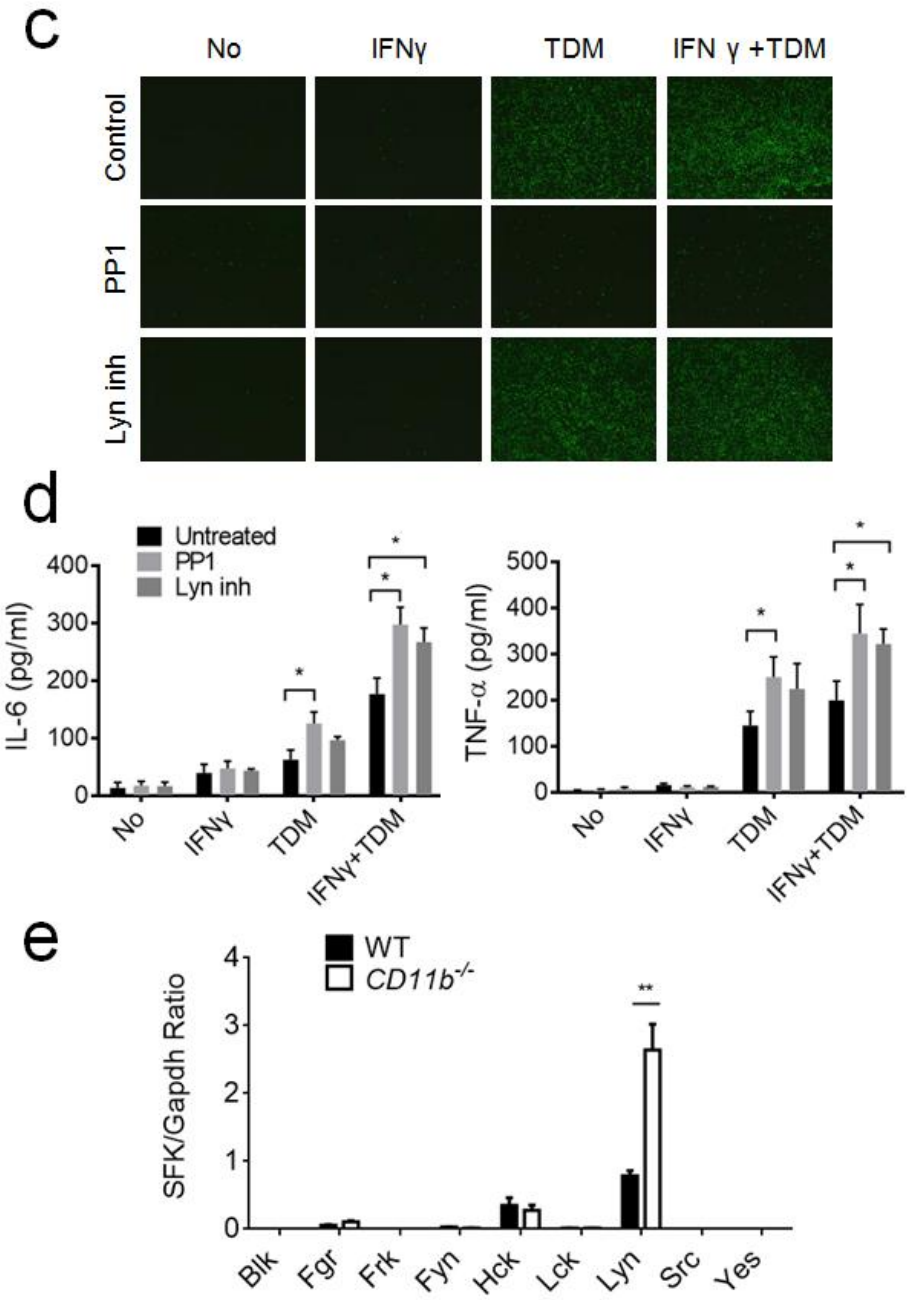

- continued Figure 10.

Figure 10. Lyn inhibits Mincle signaling by interfering with Mincle downstream target.

(**a**) IL-6 cytokine production in the culture supernatants from WT BMMs that were treated with TDM and the indicated inhibitors for 24 h was measured by ELISA. (**b**) Syk and Erk kinase activation in WT BMM that were treated with TDM and either DMSO or PP1 for 6 h were analyzed by western blot. (**c**) WT and *CD11b*$^{-/-}$ BMMs were stimulated with TDM for 24 h, and then the mRNA levels of Src family kinases (SFK) were quantified by qRT-PCR. (**d**) Knockout of *Lyn* in iBMMs was confirmed using western blot (right panel). WT and *Lyn*-knockout iBMMs were stimulated with TDM. After 24 h of stimulation, cytokine production of IL-6 and TNF-α was detected by ELISA. (**e**) Phosphorylation of Syk and Erk after 0, 3, or 24 h of TDM stimulation was compared by western blot assay. β-actin protein expression was used as loading control in western blot assay Data are representative of at least three (**a**, **c** and **e** upper panel) or two (**b, d and e** lower panle) independent experiments. **P*<0.05, ***P*<0.01, ****P*<0.0001 (two-tailed unpaired Student's t-test).

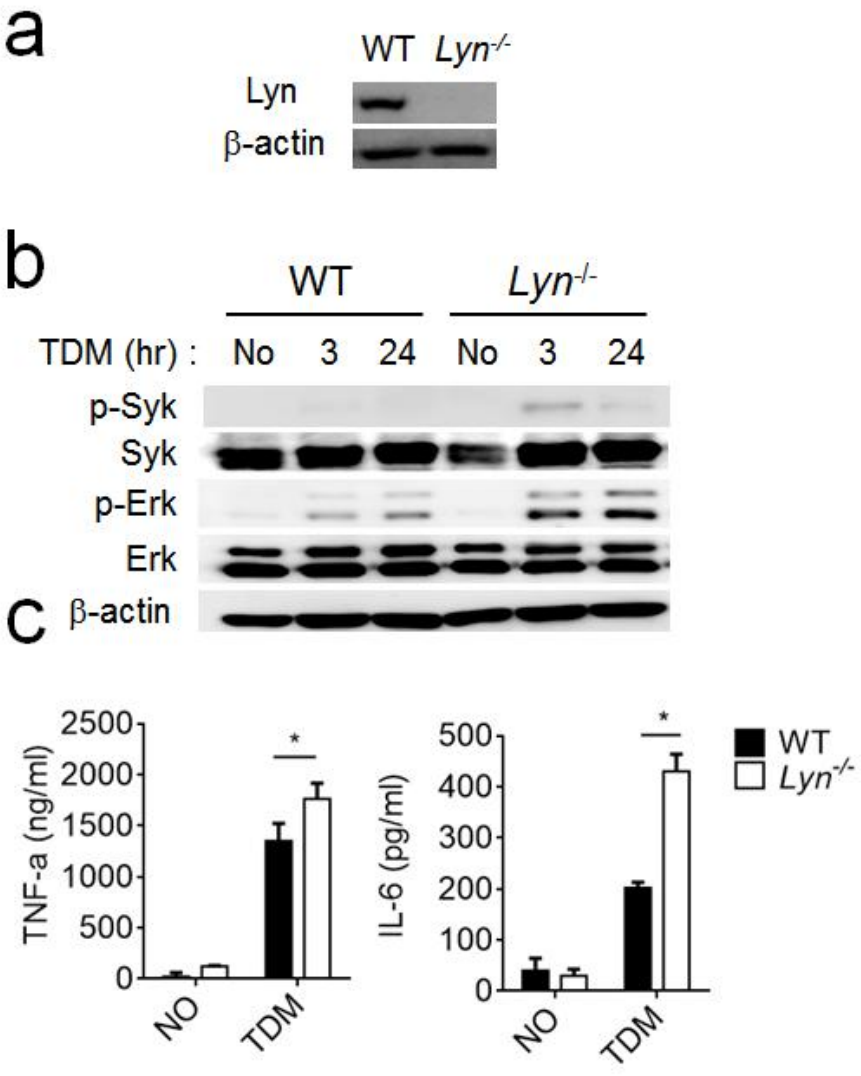

Figure 11. Enhanced Mincle signaling and cytokine production in Lyn$^{-/-}$ iBMMs.

Figure 11. Enhanced Mincle signaling and cytokine production in Lyn$^{-/-}$ iBMMs.

(**a**) Knockout of Lyn in iBMMs was confirmed by western blot. WT and Lyn$^{-/-}$ iBMMs were stimulated with TDM. (**b**) After 24 h of stimulation, levels of IL-6 and TNF-α were determined by ELISA. (**c**) Phosphorylation of Syk and Erk after 0, 3, or 24 h of TDM stimulation was evaluated by western blot. β-actin protein expression was used as a loading control. Data are representative of at least three (**c**) or two (**a** and **b**) independent experiments. **P*<0.05 (two-tailed unpaired Student's t-test).

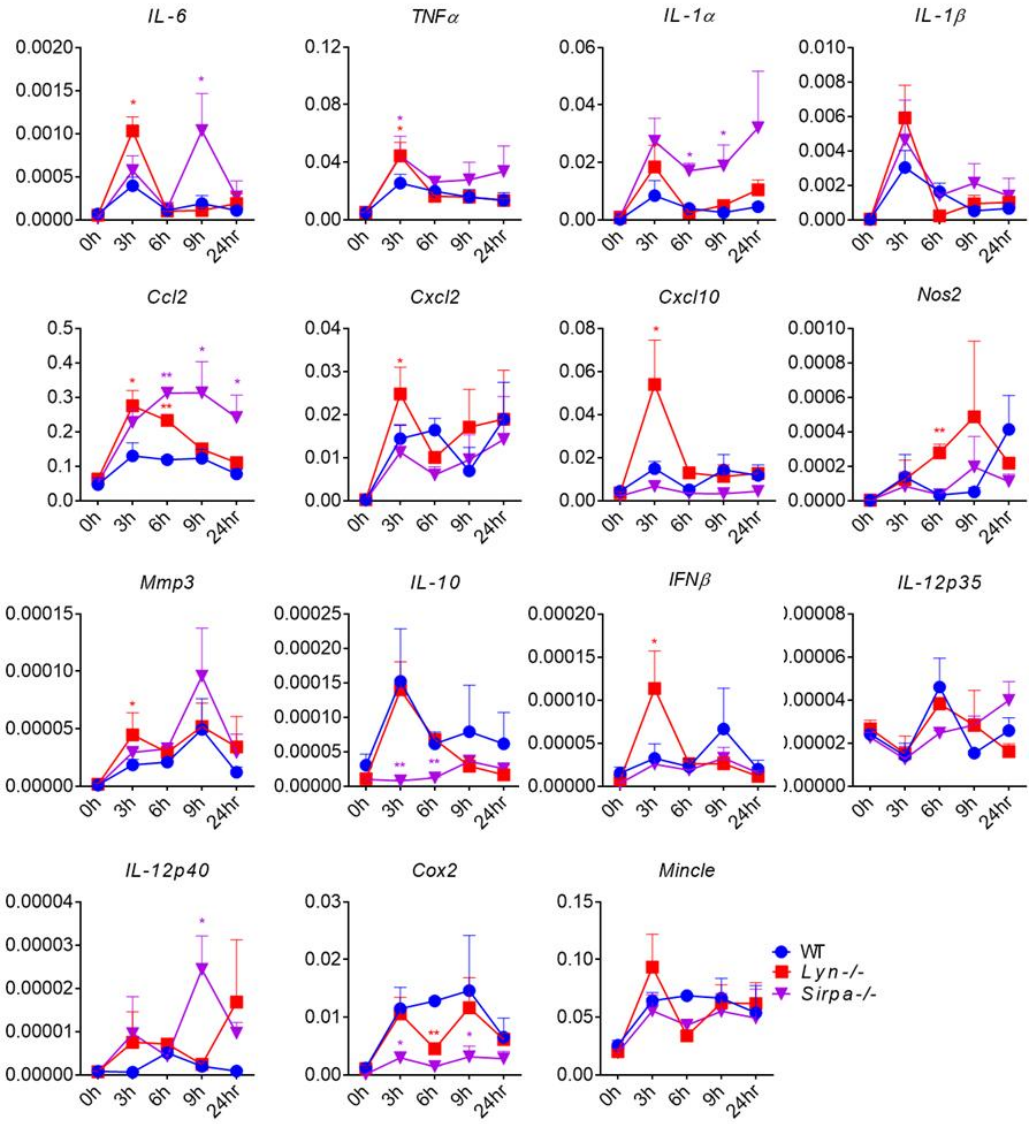

Figure 12. Induction of proinflammatory genes in WT, *Lyn*$^{-/-}$ and *Sirp*α$^{-/-}$ iBMMs upon TDM stimulation.

Figure 12. Induction of proinflammatory genes in WT, *Lyn*$^{-/-}$ and *Sirp*α$^{-/-}$ iBMMs upon TDM stimulation.

Quantitative PCR was performed on WT, *Lyn*$^{-/-}$, and *Sirp*α$^{-/-}$ iBMMs that were treated with TDM for the indicated times. Results were normalized to *Gapdh* expression. Data are representative of three independent experiments. **P*<0.05, ***P*<0.01 (two-tailed unpaired Student's *t*-test).

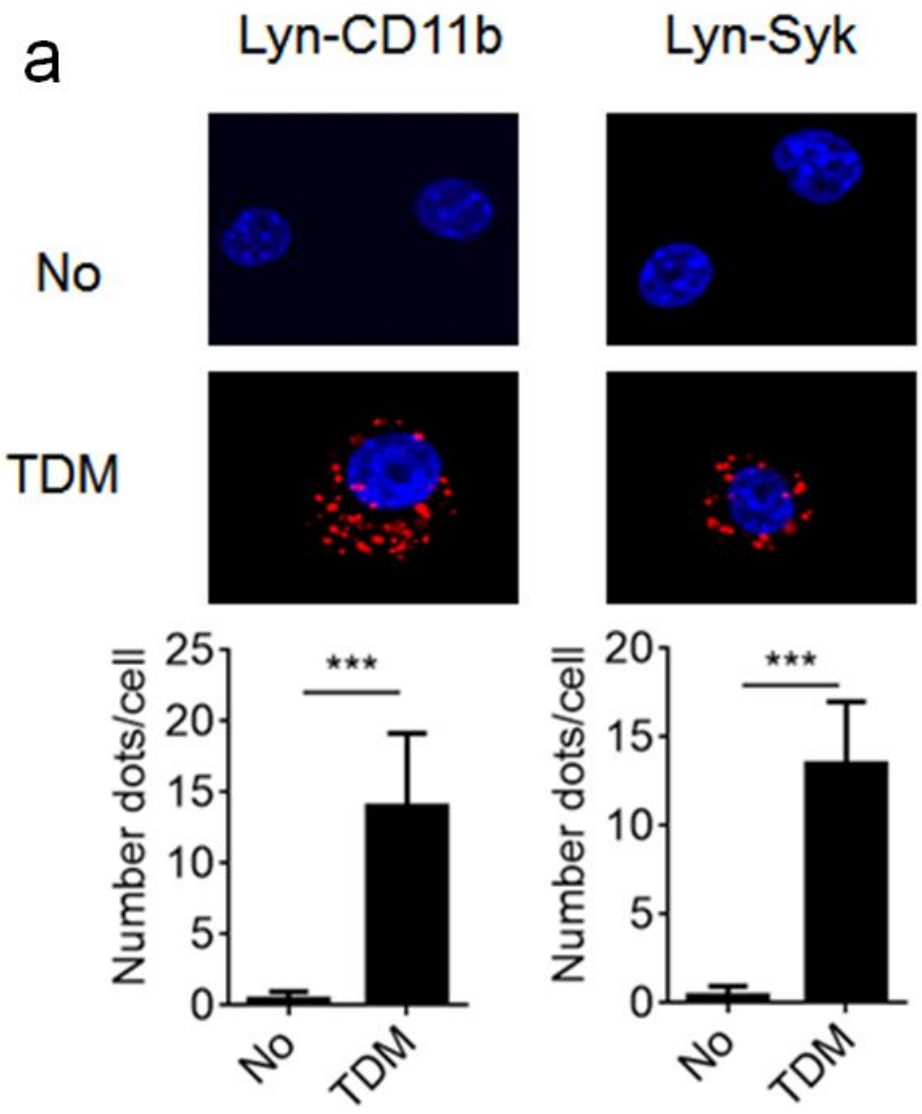

Figure 13. Lyn recruits Shp1 to dephosphorylate Syk.

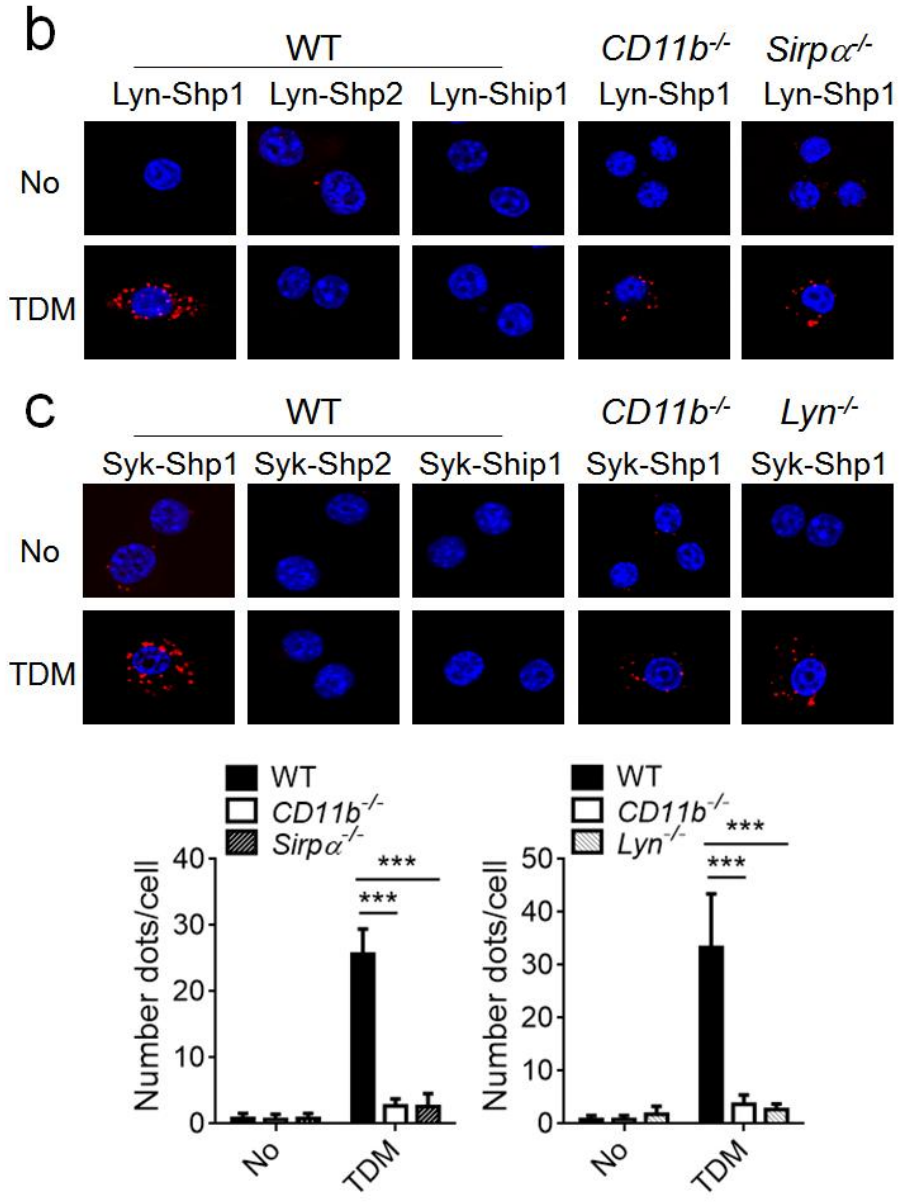

- continued Figure 13.

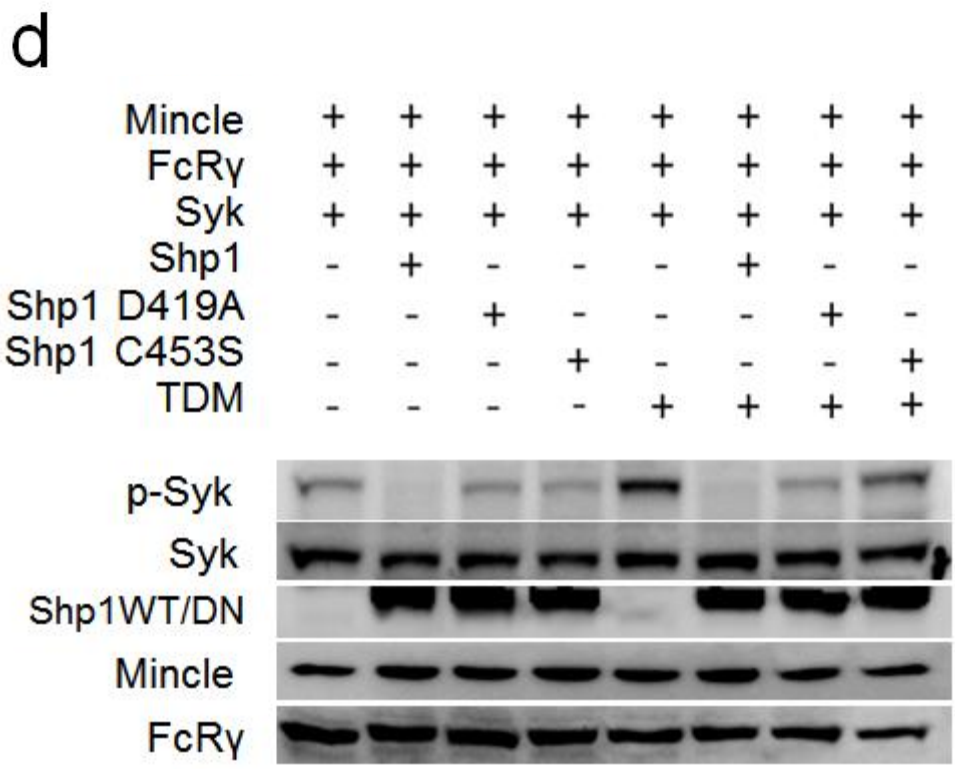

- continued Figure 13.

Figure 13. Lyn recruits Shp1 to dephosphorylate Syk.

iBMMs were transfected with Flag-CD11b and HA-Lyn or, HA-Lyn and Flag-Syk for (**a**), HA-lyn and Myc-Shp1 or Myc-Shp2 or Myc-Ship1 for (**b**), Flag-Syk and Myc-Shp1 or Myc-Shp2 or Myc-Ship1 for (c) for 24 h, followed by stimulation with TDM for 12 h before assessed with the PLA assay. (**a**) Interaction of Lyn to CD11b or Syk was measured by PLA assay. (**b** and **c**) Specific binding of Lyn and Syk to Shp1, Shp2, and Ship1 in iBMMs was examined. Interactions were visualized as fluorescent spots (Red, PLA signal), nuclei were stained with DAPI (blue), and the number of PLA signals was determined for at least 50 cells for each condition. (**d**) Immunoblot analysis of 293T cells that were transiently transfected with V5-Mincle, Myc-FcRγ, Flag-Syk together with Flag tagged WT or phosphatase-inactive Shp-1 (C453S or D419A) for 24 h. Cells were then treated with or without TDM for 6 h. Data are representative of three independent experiments. ***P<0.0001 (two-tailed unpaired Student's t-test).

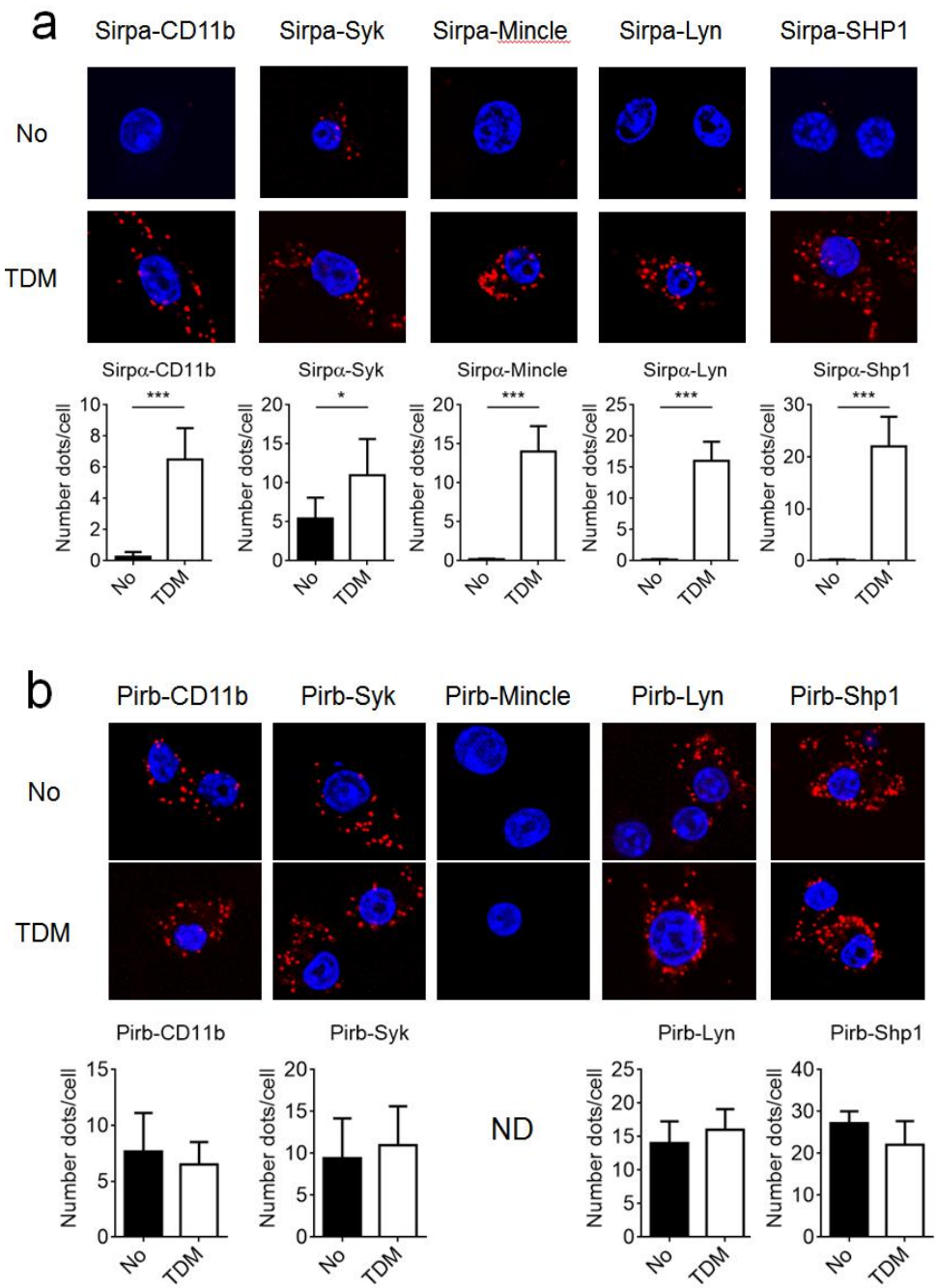

Figure 14. ITIM motif-containing Sirpα is critical for Shp1 docking and interaction with Syk

Figure 14. ITIM motif-containing Sirpα is critical for Shp1 docking and interaction with Syk

(**a**) iBMM cells were transfected with one of Flag-CD11b, Flag-Syk, V5-Mincle, HA-Lyn, Flag-Shp1 for 24 h and then treated with TDM for 24 h before assessment with the PLA assay. Interaction of endogenous Sirpα with indicated proteins were visualized as fluorescent spots (Red, PLA signal), nuclei were stained with DAPI (blue), and the number of PLA signals was determined for at least 50 cells for each condition. HA-Lyn, Flag-Shp1 and the interactions of endogenous (b)Pirb with the indicated target were determined with the PLA assay. (c-e) *Lyn-/-, Sirpα-/-, Syk-/-* iBMM cells were transfected with one of Flag-CD11b, Flag-Syk, V5-Mincle, HA-Lyn, Flag-Shp1 and the interactions of endogenous *Sirpa* with the indicated target were determined with the PLA assay. Interactions were visualized as fluorescent spots (Red, PLA signal), nuclei were stained with DAPI (blue), the number of PLA signals was determined for at least 50 cells for each condition and shown at the bottom graphs. ND, not detected. Data are representative of three independent experiments. $^{**}P<0.01$, $^{***}P<0.0001$ (two-tailed unpaired Student's *t*-test).

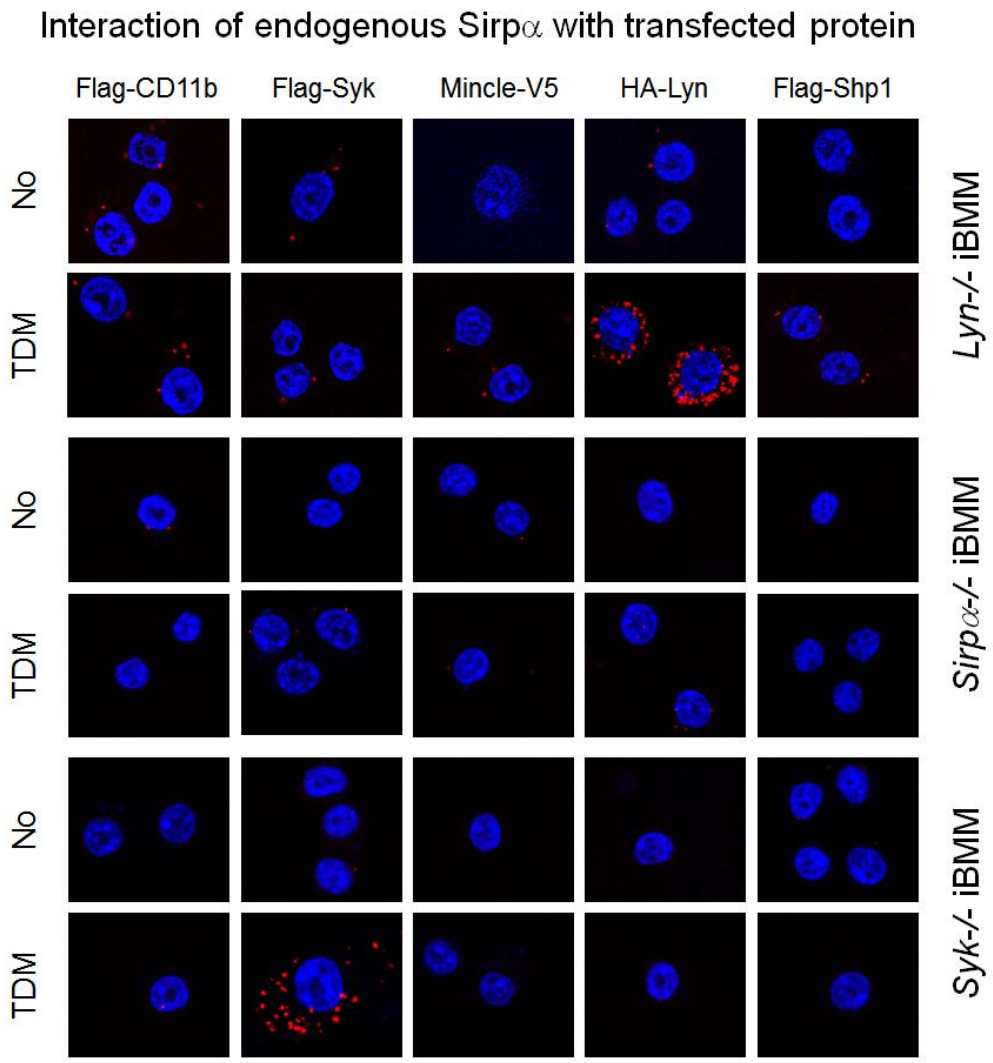

Figure 15. Interaction of SIRPα with transfected proteins in SIRPα$^{-/-}$, Lyn$^{-/-}$, and Syk$^{-/-}$ iBMMs.

Figure 15. Interaction of SIRPα with transfected proteins in SIRPα$^{-/-}$, Lyn$^{-/-}$, and Syk$^{-/-}$ iBMMs.

Lyn$^{-/-}$, SIRPα$^{-/-}$, and Syk$^{-/-}$ iBMMs were transfected separately with Flag-CD11b, Flag-Syk, V5-Mincle, HA-Lyn, and Flag-SHP1, and the interactions between endogenous SIRPα and the indicated targets were determined by PLA assay. Interactions were visualized as fluorescent spots (red, PLA signal), and nuclei were stained with DAPI (blue).

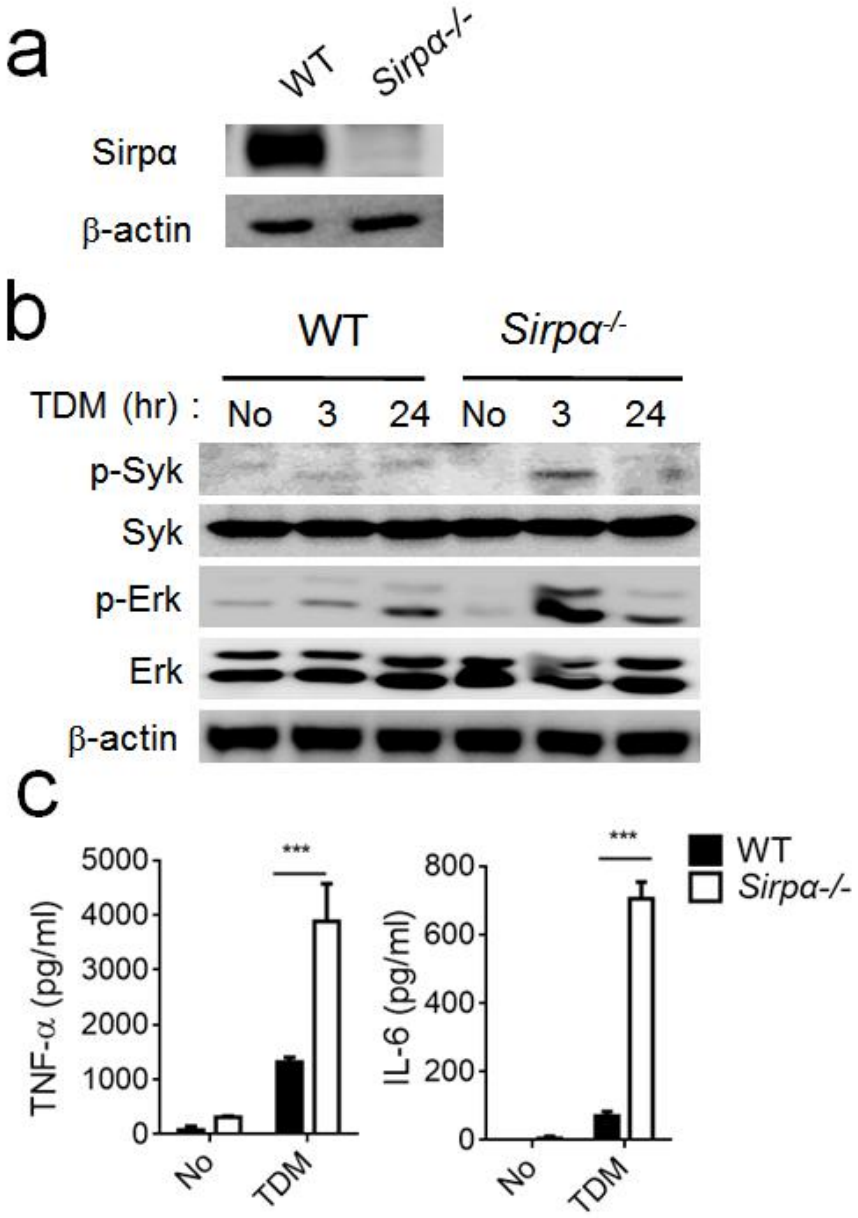

Figure 16. Sirpa displayed negative role in Mincle signal regulation

Figure 16. Sirpa displayed negative role in Mincle signal regulation

(a) Sirpα knock out was confirmed by western blot assay (top panel). Culture media were collected 24 h after TDM stimulation and subjected to ELISA for measurement of IL-6 and TNF-α production (bottom panel). (**b**) WT and Sirpα-deficient iBMMs were stimulated with TDM for the indicated times. (**c**)Then the kinase activity of Syk and Erk in cell lysates were determined by western blot assay. β-actin protein expression was used as loading control in western blot assay. Data are representative of two (**a** and **b**) or three **(c)** independent experiments. **P*<0.05, ****P*<0.0001 (two-tailed unpaired Student's *t*-test).

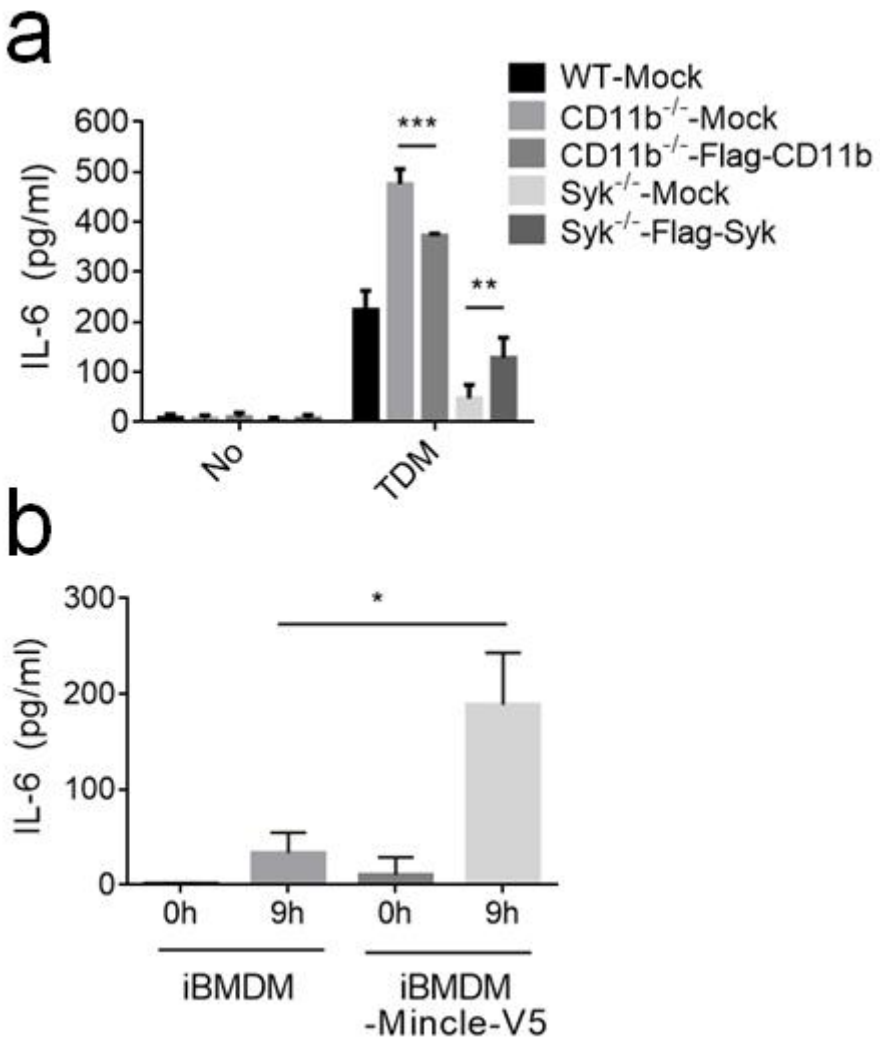

Figure 17. IL-6 production in Mincle-expressing iBMMs, and rescue experiments with CD11b$^{-/-}$ and Syk$^{-/-}$ iBMMs.

Figure 17. IL-6 production in Mincle-expressing iBMMs, and rescue experiments with CD11b$^{-/-}$ and Syk$^{-/-}$ iBMMs.

(**a**) WT iBMMs and iBMMs stably expressing Mincle-V5 were treated with TDM for 9 h, and IL-6 production was assayed by ELISA. (**b**) CD11b$^{-/-}$ iBMMs transiently transfected with Flag-CD11b and Syk$^{-/-}$ iBMMs transiently transfected with Flag-Syk were stimulated with TDM for 24 h. IL-6 secretion was determined by ELISA. Data are representative of three independent experiments.

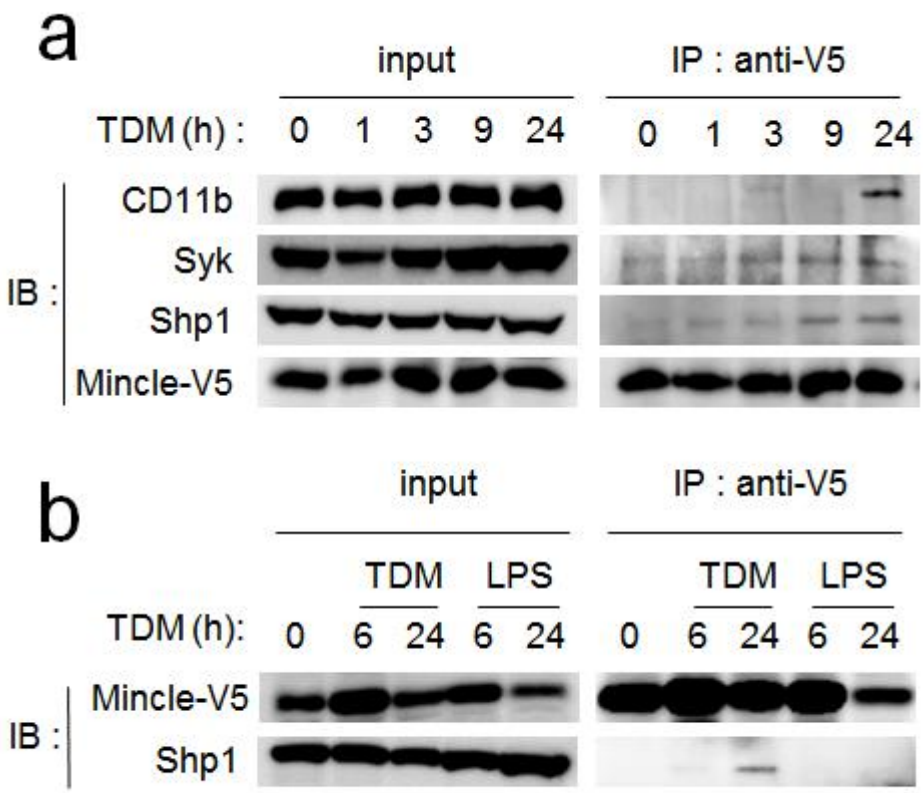

Figure 18. Complex formation of CD11b with Mincle upon TDM stimulation

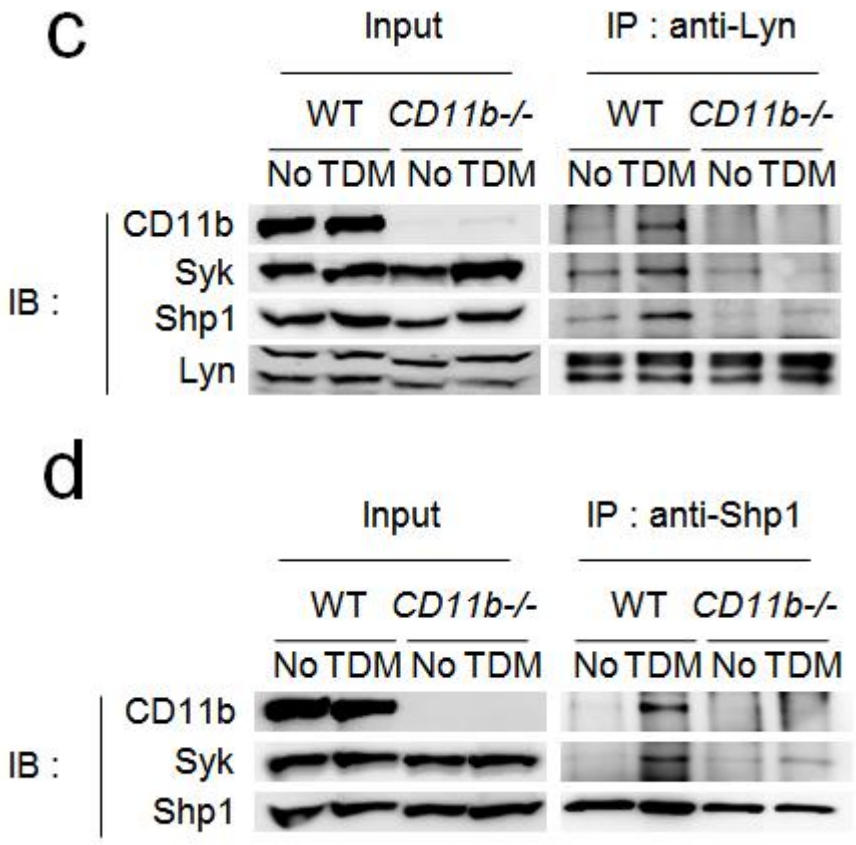

- continued Figure 18

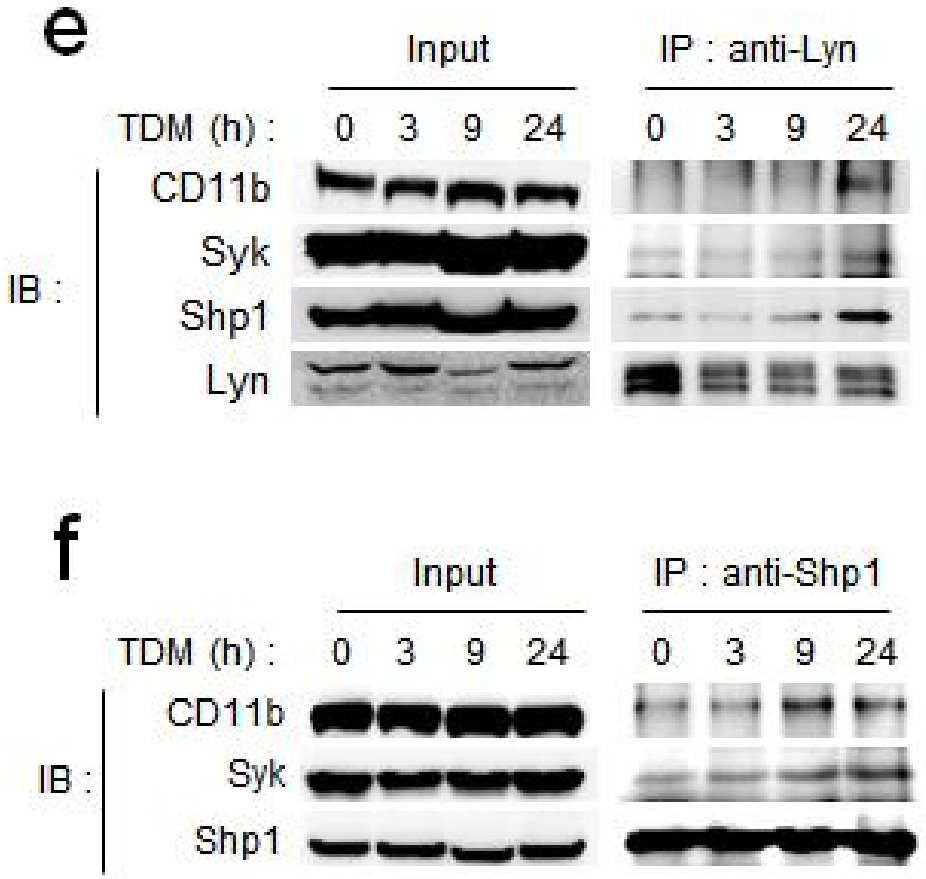

- continued Figure 18

Figure 18. Complex formation of CD11b with Mincle upon TDM stimulation

(a and b) After immunoprecipitation with Mincle in TDM or LPS stimulated Mincle stable expression iBMM cells, Mincle-V5, CD11b, Syk and Shp1 were assayed with WB (c and d) Immunoprecipitation of endogenous Lyn in WT and CD11b-/- BMMs upon TDM stimulation, Shp1, CD11b and Syk were assayed with WB at **(c)** indicated times or **(e)** 24 h after stimulation. **(d and f)** Immunoprecipitation of endogenous Shp1 in WT and CD11b-/- BMMs upon TDM stimulation, then Shp1 and Syk were assayed with WB at **(e)** indicated times or **(f)** 24 h after stimulation.. Data are representative of at least two independent experiments.

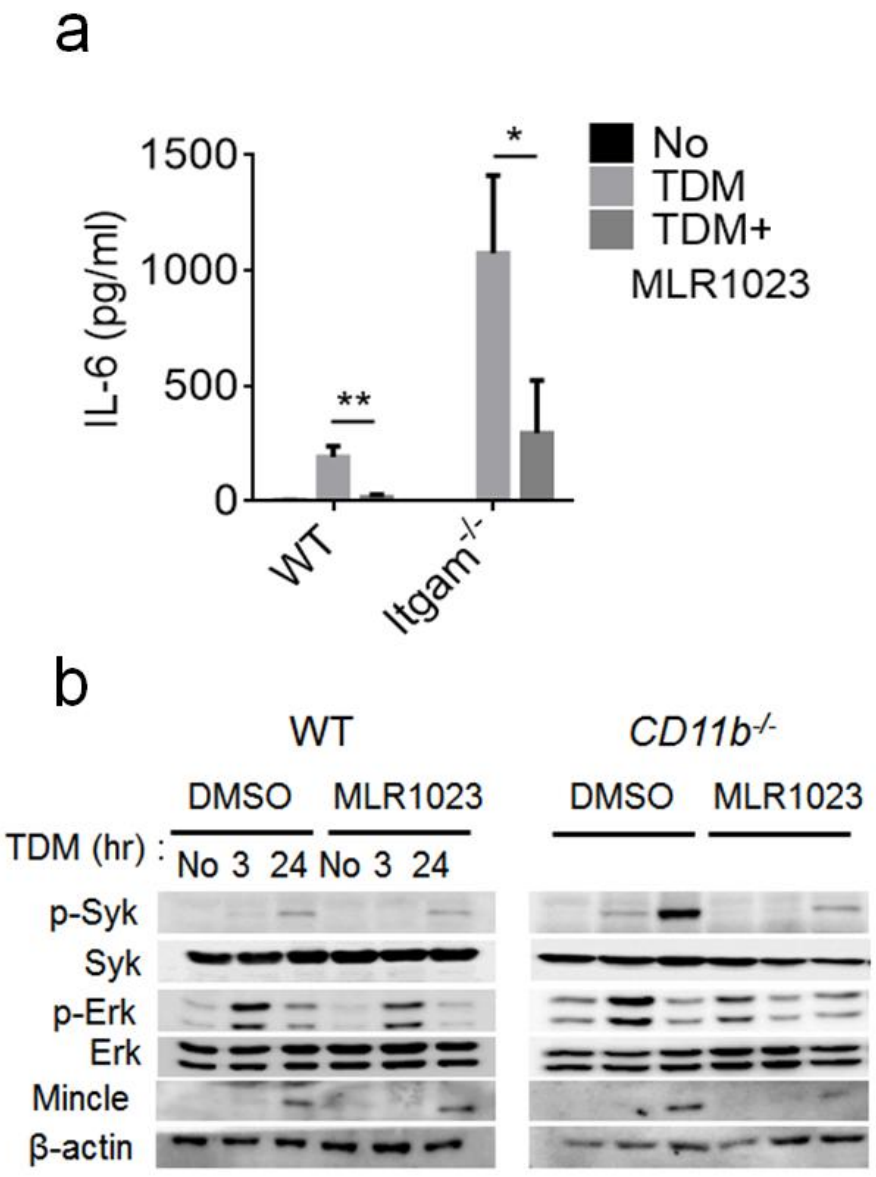

Figure 19. Lyn activator MLR1023 inhibits TDM signaling both in vivo and in vitro.

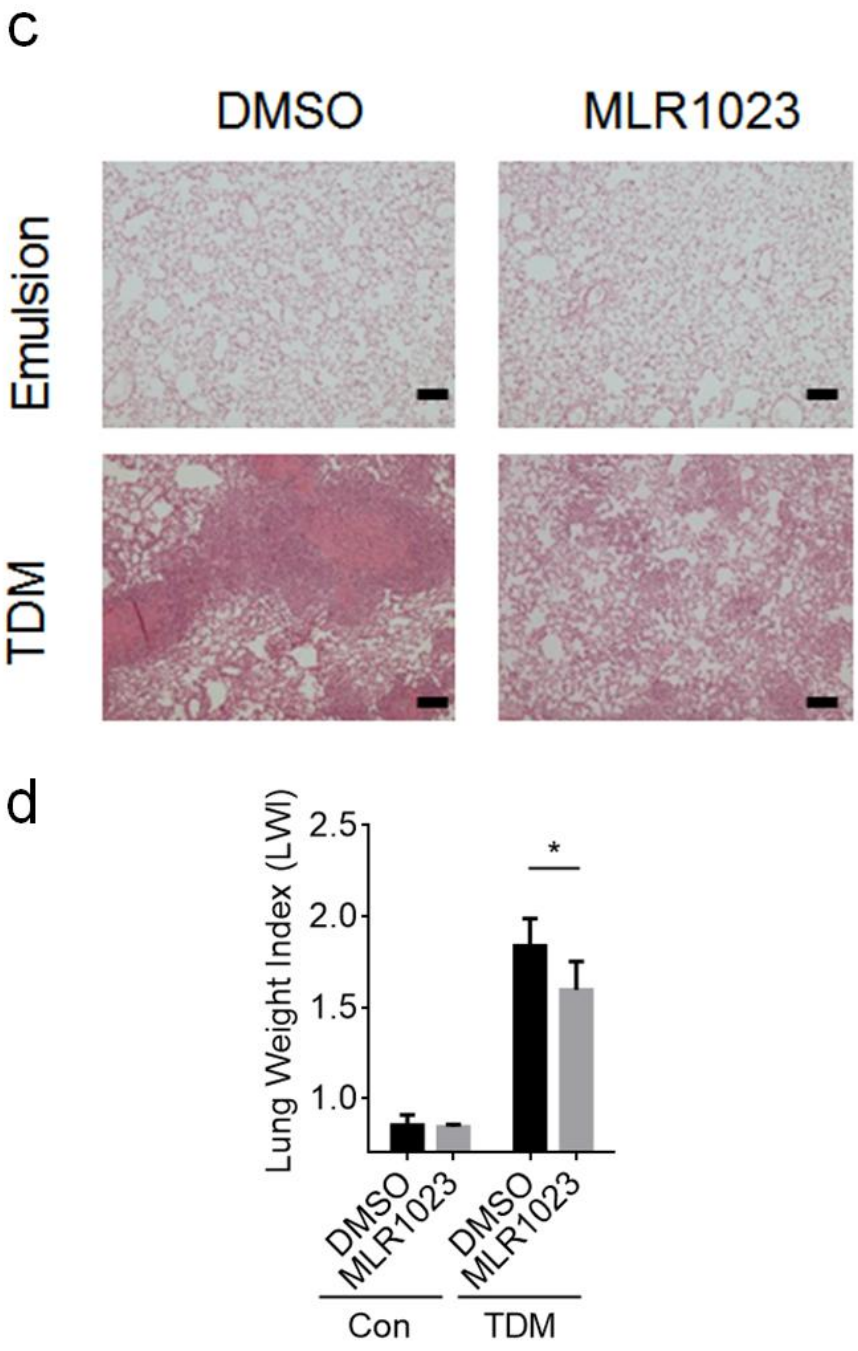

- continued Figure 19.

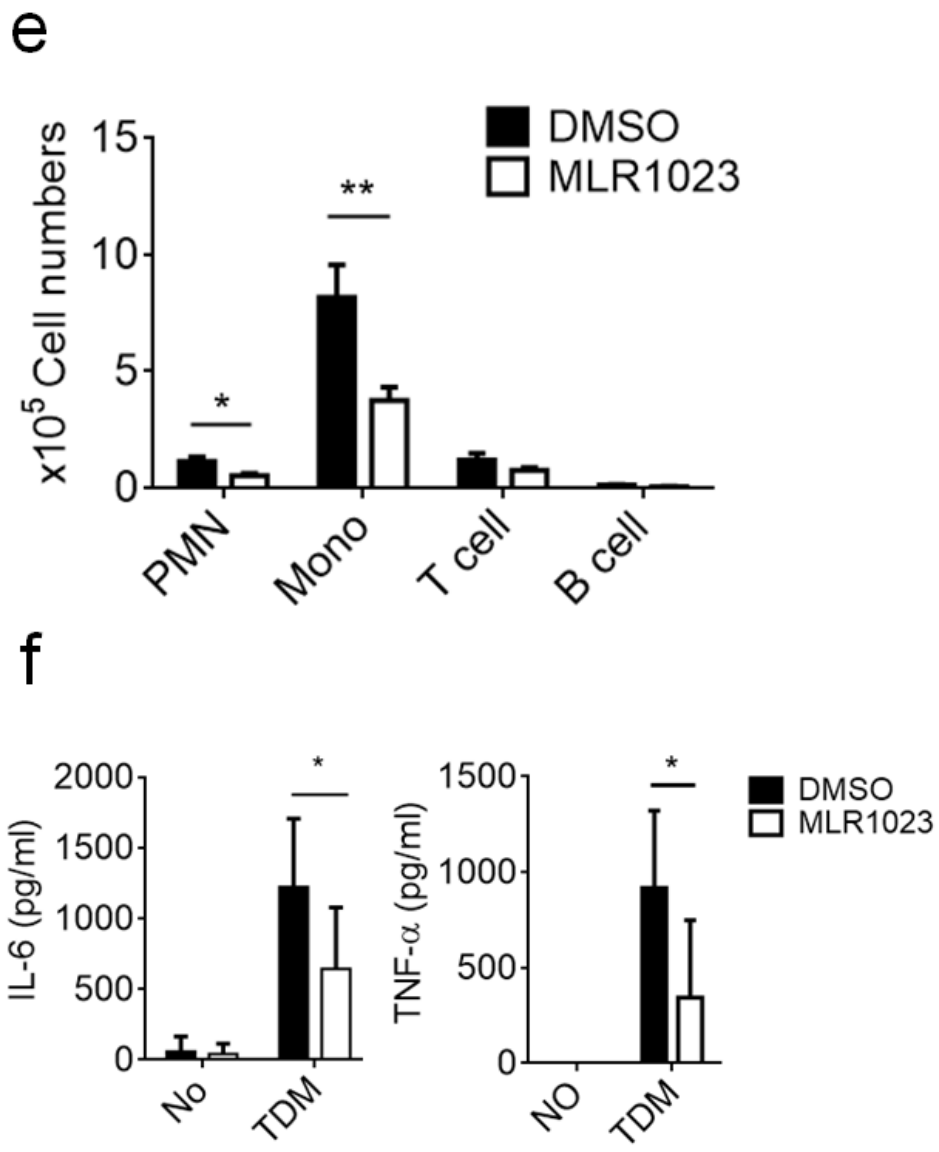

- continued Figure 19.

Figure 19. Lyn activator MLR1023 inhibits TDM signaling both in vivo and in vitro.

(**a**) Production of IL-6 by WT and *CD11b*$^{-/-}$ BMMs challenged with TDM and (1 ng/ml) MLR1023 or DMSO for 24 h was assessed by ELISA. (**b**) Western blot assay of Syk and Erk kinase activity and Mincle induction in WT and *CD11b*$^{-/-}$ BMMs challenged by TDM and (1 ng/ml) MLR1023 or DMSO for 24 h. β-actin protein expression was used as loading control in western blot assay. Experimental and control group mice (n=8) were intravenously injected with (3.75 mg/kg) TDM in an oil-in-water emulsion on Day 0. Then the treatment group mice were intraperitoneally injected with MLR1023 (6 mg/kg in PBS) every day beginning on Day 1 until the mice were sacrificed 7 d post-TDM challenge. The control group mice were injected with 1% DMSO in PBS. (**c**) Lung tissues were isolated and stained with hematoxylin and eosin (H&E) for histology analysis after the lung weight index (LWI) (**d**) was determined. (**e**) Leukocyte subsets were analyzed by flow cytometry with distinct markers for monocytes and macrophages (Mo/Ma, CD11b+ Ly6G-), neutrophils (PMN CD11b+ Ly6G+), T cells (CD3+), and B cells (CD19+). (**f**) The lung homogenates were analyzed by ELISA for TNF-α and IL-6 production. Data are

representative of two independent experiments. (**c-f**, mean and s.d. of 8 mice per group). **P*<0.05, ***P*<0.01 (two-tailed unpaired Student's *t*-test).

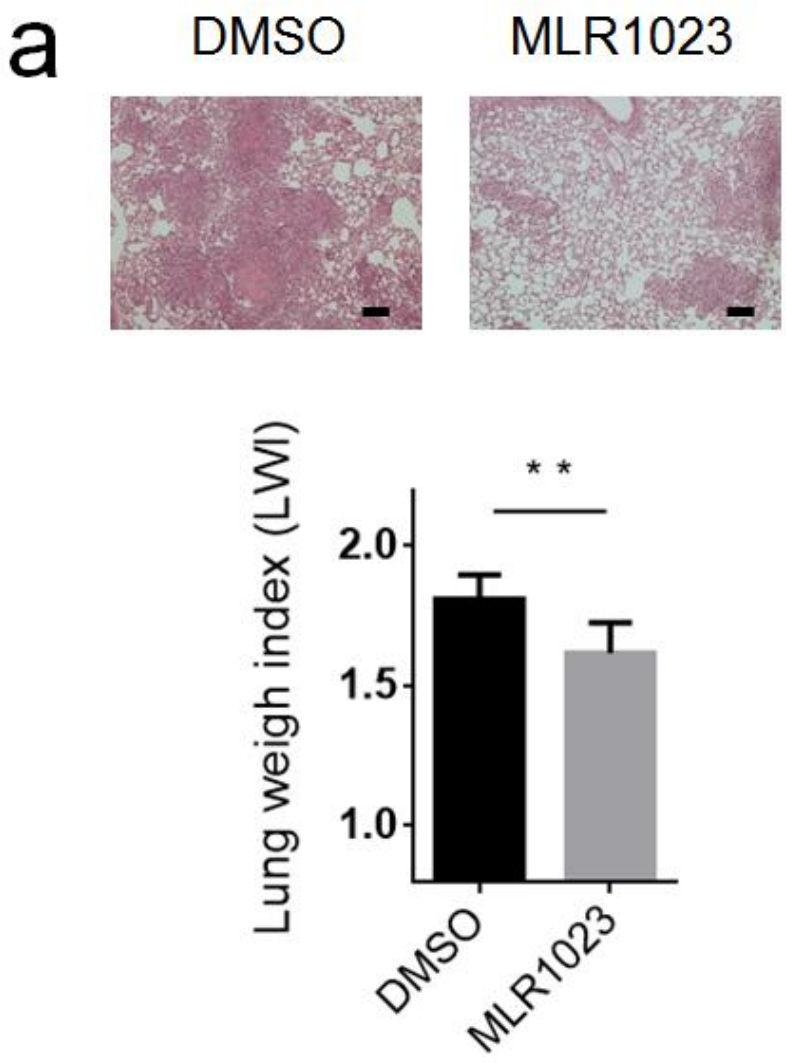

Figure 20. MLR1032 restrict granulomas response TDM injected *CD11b-/-* mice

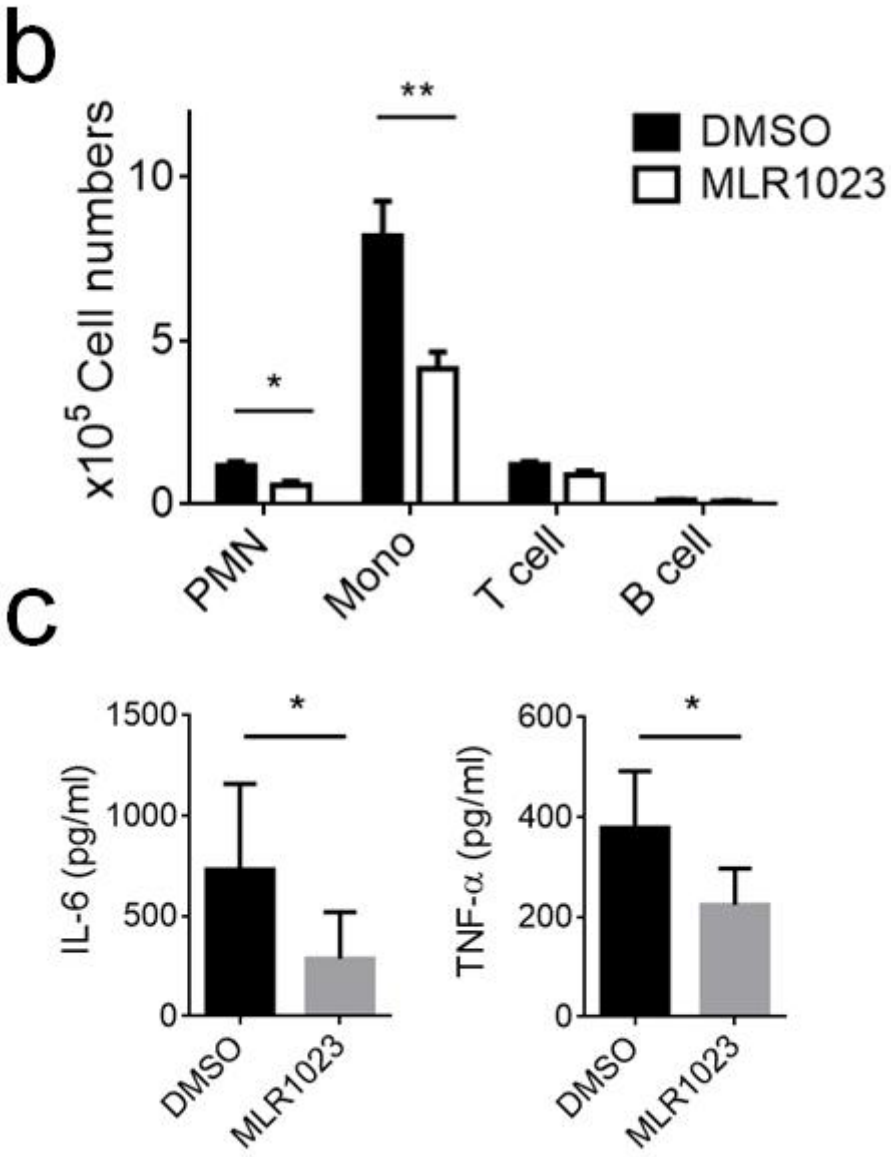

- continued Figure 20.

Figure 20. MLR1032 restricte granulomas response TDM injected *CD11b-/-* mice

Experimental and control group mice (n=7) were intravenously injected with (2 mg/kg) TDM in an oil-in-water emulsion on Day 0. Then the treatment group mice were intraperitoneally injected with MLR1023 (6 mg/kg in PBS) every day beginning on Day 1 until the mice were sacrificed 7 d post-TDM challenge. The control group mice were injected with 1% DMSO in PBS. (**a**) Lung tissues were isolated and stained with hematoxylin and eosin (H&E) for histology analysis after the lung weight index (LWI) was determined. (**b**) Leukocyte subsets were analyzed by flow cytometry with distinct markers for monocytes and macrophages (Mo/Ma, CD11b+ Ly6G-), neutrophils (PMN CD11b+ Ly6G+), T cells (CD3+), and B cells (CD19+). (c) The lung homogenates were analyzed by ELISA for TNF-α and IL-6 production. Data are representative of two independent experiments. (**a-c**, mean and s.d. of 7 mice per group). *P<0.05, **P<0.01 (two-tailed unpaired Student's t-test).

Table 1 List of PCR primers used in this study

Real time-PCR

Gene	GeneBank_ID	5'Forward sequence3'	3'Reverse sequence5'
Il-6	NM_031168	CCAAGACCATCCAATTCATC	CCACAAACTGATATGCTTAGG
TNFa	NM_013693	ATGTCCATTCCTGAGTTCTG	AATCTGGAAAGGTCTGAAGG
IL-1a	NM_010554	AGGGAGTCAACTCATTGGCG	CTTCCCGTTGCTTGACGTTG
IL-1b	NM_008361	TCAACCAACAAGTGATATTCTC	ACACAGGACAGGTATAGATTC
Cxcl2	NM_009140	CATCCCACCCACACAGTGAAAGAG	CCTTCCATGAAAGCCATCCGACTG
Ccl2	NM_011333	TTCCACAACCACCTCAAGCACTTC	TTAAGGCATCACAGTCCGAGTCAC
Cxcl10	NM_021274	TCGCTCAAGTGGCTGGGATGG	GGGCATGGCACATGGTGAAGG
Nos2	NM_010927	AATCTTGGAGCGAGTTGTGG	CAGGAAGTAGGTGAGGGCTTG
Mincle	NM_019948	AGTGAGGCATCAGGTTCAGTCAAG	GACCAGGTCAAGGTTGTCGTAGAG
Cox-2	NM_011198	GCCCGTGCTGCTCTGTCTTAAC	GTTGCTCTAGGCTTTGCTGGCTAC
Mmp3	NM_010809	CTCATGCCTATGCACCTGGA	GGCTGAGTGGTAGAGTCCCA
IL-12p35	NM_001159424	TTTGATGATGACCCTGTGCCTTGG	GATTCTGAAGTGCTGCGTTGATGG
IL-12p40	NM_001303244	AGTAAAGACATAGGTGGTATTTG	CTGGTTTCTTATCAATATCACTTC
IL-10	NM_010548	GCACTACCAAAGCCACAAAGCAG	GTCAGTAAGAGCAGGCAGCATAGC
IFNb	NM_010510	CCACTTGAAGAGCTATTACTG	AATGATGAGAAAGTTCCTGAAG
Src	NM_009271	CGCCTCACTACCGTATGTCC	CAACACCCGGAAGCCTAGAG
Yes	NM_009535	CGGCAAGACAAGGTGCAAAA	CCTGTGGAGTAACAGCCAAGT
Fyn	NM_001122893	GCCACATAGCTACAGGACCG	AATCACAGTTCGCTGGAGCA
Fgr	NM_010208	GCTGGAAGTTAGGGTTGGCT	GCCTCATAGTCGTACAGGGC
Lck	NM_001162432	ATGGAGAACGGGAGCCTAGT	GACACGCATCAATCGCAGAC
Hck	NM_001172117	CCTCCGAGATGGAAGCAAGG	GCCACTTTGGTGTGCTTGTT
Blk	NM_007549	GCCCCAGTAGAGACTCTGGA	GCCTGGGGATTTCCCATTCA
Lyn	NM_001111096	AGGAAGAACACCCTGGATGC	CATTTTCTGGGGGTTGTGCG
Frk	NM_001159544	CTATTGTGCGGCACCGAATG	AGGCAAAGGTGTCCCAAACA
Gapdh	NM_008084	GGCAAATTCAACGGCACAGTCAAG	TCGCTCCTGGAAGATGGTGATGG

Site-directed mutagenesis

Mutation		Primer sequence
Shp1 DN C453S	Forward	GGCCCATCATTGTGCATAGCAGCGCTGGCATCGGCC
	Reverse	GGCCGATGCCAGCGCTGCTATGCACAATGATGGGCC
Shp1 DN D419A	Forward	AGTACCTGAGCTGGCCTGCCCATGGGGTTCCCAGTGAG
	Reverse	CTCACTGGGAACCCCATGGGCAGGCCAGCTCAGGTACT

Crispr-Cas9 gRNA

Gene	5'Forward sequence3'	3'Reverse sequence5'
CD11b	CACCGCTTGTGTCATGGCTTCAATC	AAACGATTGAAGCCATGACACAAGC
Lyn	CACCGGTTCGGTCAGTATTACGTAC	AAACGTACGTAATACTGACCGAACC
Sirpα	CACCGCCGCGGCCCATGGAGCCCGC	AAACGCGGGCTCCATGGGCCGCGGC
Syk	CACCGTATTGCACTACCGCATTGAC	AAACGTCAATGCGGTAGTGCAATAC

-Continued Table 1

Cloning

Plasmid		Primer sequence	Restriction Enzyme
pCS4-3×flag-shp1	Forward	AATGAATTCAATGGTGAGGTGGTTTCA	EcoRI
	Reverse	ATTCTCGAGTCACTTCCTCTTGAGAGAAC	XhoI
pCS2-6×myc-shp2	Forward	AGTGAATTCAATGACATCGCGGAGAT	EcoRI
	Reverse	TGATCTAGATCATCTGAAACTCCTCTGCT	XbaI
pCS2-6×myc-ship1	Forward	ATTGAATTCAATGCCTGCCATGGT	EcoRI
	Reverse	AAACTCGAGTCACTGCATGGCAGTC	XhoI
pCS4-3×flag-syk	Forward	AATGAATTCAATGGCGGGAAGTG	EcoRI
	Reverse	ATTCTCGAGTTAGTTAACCACGTCGTAGT	XhoI
pCS4-3×flag-CD11b	Forward	AAATCTAGATATGACTCTTAAAGCTCTTCT	XbaI
	Reverse	ATAGCTAGCTTACTGAGGTGGG	NheI
pCS4-3×flag-CD18	Forward	ATTGAATTCAATGCTGGGCCCACACT	EcoRI
	Reverse	AAACTCGAGCTAGCTTTCAGCAAACTT	XhoI
pCS4-3×HA-Lyn	Forward	GCGAGATCTGGATGGGATGTATTAAATC	BglII
	Reverse	ATTCTCGAGCTACGGTTGCTGCTGA	XhoI
pcDNA3.1-MincleV5	Forward	CCCGATCCACCATGAATTCAACCAAATCGCCTG	BamHI
	Reverse	CCGCTCGAGGTCCAGAGGACTTATTTCTGGCAT	XhoI
pcDNA4-FceR1g-Myc	Forward	CCCAAGCTTATGATCTCAGCCGTGATCTT	HindIII
	Reverse	CGCCTCGAGCTGGGGTGGTTTCTCATGCTT	XhoI

References

1. Cosma, C.L., Sherman, D.R. & Ramakrishnan, L. The secret lives of the pathogenic mycobacteria. *Annu Rev Microbiol* **57**, 641-676 (2003).

2. Davis, J.M. & Ramakrishnan, L. The role of the granuloma in expansion and dissemination of early tuberculous infection. *Cell* **136**, 37-49 (2009).

3. Ramakrishnan, L. Revisiting the role of the granuloma in tuberculosis. *Nat Rev Immunol* **12**, 352-366 (2012).

4. Saunders, B.M. & Cooper, A.M. Restraining mycobacteria: Role of granulomas in mycobacterial infections. *Immunol. Cell Biol.* **78**, 334–341 (2000).

5. Sasindran, S.J. & Torrelles, J.B. Mycobacterium Tuberculosis Infection and Inflammation: what is Beneficial for the Host and for the Bacterium? *Front Microbiol* **2**, 2 (2011).

6. Cavalcanti, Y.V., Brelaz, M.C., Neves, J.K., Ferraz, J.C. & Pereira, V.R. Role of TNF-Alpha, IFN-Gamma, and IL-10 in the Development of Pulmonary Tuberculosis. *Pulm Med* **2012**, 745483 (2012).

7. Song, C. *et al.* IL-17-Producing Alveolar Macrophages Mediate Allergic Lung Inflammation Related to Asthma. *The Journal of Immunology* **181**, 6117-6124 (2008).

8. Redford, P.S., Murray, P.J. & O'Garra, A. The role of IL-10 in immune regulation during M. tuberculosis infection. *Mucosal Immunol* **4**, 261-270 (2011).

9. Ishikawa, E. *et al.* Direct recognition of the mycobacterial glycolipid, trehalose dimycolate, by C-type lectin Mincle. *J Exp Med* **206**, 2879-2888 (2009).

10. Baba, T., Natsuhara, Y., Kaneda, K. & Yano, I. Granuloma formation activity and mycolic acid composition of mycobacterial cord factor. *Cell. mol. life sci.* **53**, 227-232 (1997).

11. Lang, R. Recognition of the mycobacterial cord factor by Mincle: relevance for granuloma formation and resistance to tuberculosis. *Front Immunol* **4**, 5 (2013).

12. Lee, W.B. *et al.* Neutrophils Promote Mycobacterial Trehalose Dimycolate-Induced Lung Inflammation via the Mincle Pathway. *PLoS Pathog* **8**, e1002614 (2012).

13. Luo, B.H., Carman, C.V. & Springer, T.A. Structural basis of integrin regulation and signaling. *Annu Rev Immunol* **25**, 619-647 (2007).

14. Han, C. *et al.* Integrin CD11b negatively regulates TLR-triggered inflammatory responses by activating Syk and promoting degradation of MyD88 and TRIF via Cbl-b. *Nat Immunol* **11**, 734-742 (2010).

15. Ehirchiou, D. *et al.* CD11b facilitates the development of peripheral tolerance by suppressing Th17 differentiation. *J Exp Med* **204**, 1519-1524 (2007).

16. Ding, C. *et al.* Integrin CD11b negatively regulates BCR signalling to maintain autoreactive B cell tolerance. *Nat Commun* **4**, 2813 (2013).

17. Grees L.C. *et al.* Analysis of nitrate, nitrite, and [15N]nitrate in biological fluids. *Anal. Biochem.* **126** (1982).

18. Perez RL, Roman J, Roser S, Little C & Olsen M. Cytokine message and protein expression during lung granuloma formation and resolution induced by the mycobacterial cord factor trehalose-6,6'-dimycolate. *J Interferon Cytokine Res* **20**, 795–804 (2000).

19. Yarkoni E & HJ, R. Granuloma formation in lungs of mice after intravenous administration of emulsified trehalose-6,6'-dimycolate (cord factor): reaction intensity depends on size distribution of the oil droplets. *Infect Immun* **18**, 552-554 (1977).

20. Fossati-Jimack, L. *et al.* Phagocytosis is the main CR3-mediated function affected by the lupus-associated variant of CD11b in human myeloid cells. *PLoS One* **8**, e57082 (2013).

21. Ling, G.S. *et al.* Integrin CD11b positively regulates TLR4-induced signalling pathways in dendritic cells but not in macrophages. *Nat Commun* **5**, 3039 (2014).

22. Lee, W.B. *et al.* Mincle-mediated translational regulation is required for strong nitric oxide production and inflammation resolution. *Nat Commun* **7**, 11322 (2016).

23. Schoenen, H. *et al.* Differential control of Mincle-dependent cord factor recognition and macrophage responses by the transcription factors C/EBPbeta and HIF1alpha. *J Immunol* **193**, 3664-3675 (2014).

24. Sakaguchi, I., Tsujimura, M., Ikeda, N. & Minamino, M. Granulomatous tissue formation of shikon and shikonin by air pouch method. *Biol. Pharm. Bull.* **24**, 650-655 (2001).

25. Yamasaki, S. *et al.* Mincle is an ITAM-coupled activating receptor that senses damaged cells. *Nat Immunol* **9**, 1179-1188 (2008).

26. Zhang, Y. & Wang, H. Integrin signalling and function in immune cells. *Immunology* **135**, 268-275 (2012).

27. Harder, K.W. *et al.* Perturbed myelo/erythropoiesis in Lyn-deficient mice is similar to that in mice lacking the inhibitory phosphatases SHP-1 and SHIP-1. *Blood* **104**, 3901-3910 (2004).

28. Takai, T. & Ono, M. Activating and inhibitory nature of the murine paired immunoglobulin-like receptor family. *Immunological reviews* **181**, 215-222 (2001).

29. Barclay, A.N. & Brown, M.H. The SIRP family of receptors and immune regulation. *Nat Rev Immunol* **6**, 457-464 (2006).

30. Yassin R.J & A.S., H. Altered expression of CD11 CD18 on the peripheral blood phagocytes of patients with tuberculosis. *Clin Exp Immunol* **97**, 120-125 (1994).

31. Basu, J., Shin, D.M. & Jo, E.K. Mycobacterial signaling through toll-like

receptors. *Front Cell Infect Microbiol* **2**, 145 (2012).

32. Bai, Y. *et al.* Integrin CD11b negatively regulates TLR9-triggered dendritic cell cross-priming by upregulating microRNA-146a. *J Immunol* **188**, 5293-5302 (2012).

33. Kawai, T. & Akira, S. Signaling to NF-kappaB by Toll-like receptors. *Trends Mol Med* **13**, 460-469 (2007).

34. Schoenen, H. *et al.* Cutting edge: Mincle is essential for recognition and adjuvanticity of the mycobacterial cord factor and its synthetic analog trehalose-dibehenate. *J Immunol* **184**, 2756-2760 (2010).

35. Xu, G., Wang, J., Gao, G.F. & Liu, C.H. Insights into battles between Mycobacterium tuberculosis and macrophages. *Protein Cell* **5**, 728-736 (2014).

36. B.K. Das *et al.* Characterization of a Protein Complex Containing Spliceosomal Proteins SAPs 49, 130, 145, and 155. *Mol. Cell. Biol.* **19**, 6796–6802 (1999).

37. Scapini, P., Pereira, S., Zhang, H. & Lowell, C.A. Multiple roles of Lyn kinase in myeloid cell signaling and function. *Immunological reviews* **228**, 23-40 (2009).

38. Campbell, K.S. Signal transduction from the B cell antigen-receptor. *Curr.Opin. Immunol.* **11**, 256-264 (1999).

39. Ban, T. *et al.* Lyn Kinase Suppresses the Transcriptional Activity of IRF5 in the TLR-MyD88 Pathway to Restrain the Development of Autoimmunity. *Immunity* (2016).

40. Harder K, W. *et al.* Gain- and loss-of-function Lyn mutant mice define a critical inhibitory role for Lyn in the myeloid lineage. *Immunity* **15**, 603-615 (2001).

41. Abram, C.L. & Lowell, C.A. The diverse functions of Src family kinases in macrophages. *Frontiers in bioscience : a journal and virtual library* **13**, 4426-4450 (2008).

42. Saporito, M.S., Ochman, A.R., Lipinski, C.A., Handler, J.A. & Reaume, A.G. MLR-1023 is a potent and selective allosteric activator of Lyn kinase in vitro that improves glucose tolerance in vivo. *J Pharmacol Exp Ther* **342**, 15-22 (2012).

43. Tanaka, M. *et al.* Macrophage-inducible C-type lectin underlies obesity-induced adipose tissue fibrosis. *Nat Commun* **5**, 4982 (2014).

44. Sun, K., Tordjman, J., Clement, K. & Scherer, P.E. Fibrosis and adipose tissue dysfunction. *Cell Metab* **18**, 470-477 (2013).

45. Santon M, C. *et al.* Inflammatory Signals shift from adipose to liver during high fat feeding and influence the development of steatohepatitis in mice. *J Inflamm* **8** (2011).

46. Lee, E.J. *et al.* Mincle Activation and the Syk/Card9 Signaling Axis Are Central to the Development of Autoimmune Disease of the Eye. *J Immunol* **196**, 3148-3158 (2016).

47. Merad, M., Sathe, P., Helft, J., Miller, J. & Mortha, A. The dendritic cell lineage: ontogeny and function of dendritic cells and their subsets in the steady state and the inflamed setting. *Annu Rev Immunol* **31**, 563-604 (2013).

48. Iborra, S. *et al.* Leishmania Uses Mincle to Target an Inhibitory ITAM Signaling Pathway in Dendritic Cells that Dampens Adaptive Immunity to Infection. *Immunity* **45**, 788-801 (2016).

49. Torigoe, T., O'Connor, R., Santoli, D. & Reed, J.C. Interleukin-3 regulates the activity of the LYN protein-tyrosine kinase in myeloid-committed leukemic cell lines. *Blood* **80**, 617-624 (1992).

50. Willingham, S.B. *et al.* The CD47-signal regulatory protein alpha (SIRPa) interaction is a therapeutic target for human solid tumors. *Proceedings of the National Academy of Sciences of the United States of America* **109**, 6662-6667 (2012).

51. Matozaki, T., Murata, Y., Okazawa, H. & Ohnishi, H. Functions and

molecular mechanisms of the CD47-SIRPalpha signalling pathway. *Trends Cell Biol* **19**, 72-80 (2009).

52. Kong, X.-N. *et al.* LPS-induced down-regulation of signal regulatory protein α contributes to innate immune activation in macrophages. *The Journal of Experimental Medicine* **204**, 2719-2731 (2007).

Abstract in Korean

Lyn-Shipα-Shp1 복합체를 통한 인테그린 CD11b 단백질의 Mincle 신호전달체계 음성적 제어

마이코박테리아 감염 시, 항염증 반응은 면역 시스템의 과도한 반응에 의한 숙주의 조직 손상을 피할 수 있도록 해준다. 하지만, 아직까지 마이코박테리아에 의한 면역반응을 특이적으로 조절하는 항염증 반응의 조절자에 대해 알려진 것은 거의 없다. 이 연구에서는 인테그린 CD11b 단백질이 마이코박테리아 cord factor 에 의해 증가하는 Mincle 신호에 대한 중요한 음성 제어자라는 것을 처음으로 밝혔다. CD11b 결핍은 마이코박테리아 감염 시 과도한 염증 반응을 일으킨다. 이 때, 마이코박테리아에 의한 Mincle 의 활성화는 Syk 신호 뿐만 아니라 CD11b 신호도 켜지게 하여 Mincle-CD11b 신호 복합체의 형성을 유도한다. 특히, 활성화된 CD11b 단백질은 Lyn, Sirpα, 그리고 Shp1 를 불러와서 복합체를 형성하고, Syk 을 탈인산화 시켜 Mincle 에 의한 염증반응을 제어한다. 뿐만 아니라, Lyn 활성제인 MLR-1023 은 효과적으로 Mincle 신호를 억제하는데, 이것은 Lyn 을

매개로 염증반응 조절의 가능성을 제시하고 있다. 이러한 결과를 통하여, CD11b 가 마이코박테리아 감염에 의한 면역 반응을 세밀하게 조절할 수 있는 새로운 역할이 있음을 밝혔다는 점에서 매우 큰 의의가 있다고 할 수 있다.

핵심 되는 말 : CD11b, Mincle, Lyn-Sirpα-Shp1 복합체